INVESTIGATION OF SURFACE ACIDIC SITES ON THE CATALYST SILICA-ALUMINA BY C-13 NUCLEAR MAGNETIC RESONANCE SPECTROSCOPY

by

Septimus H. C. Liang

B. Sc. University of Toronto, 1976

A THESIS SUBMITTED IN PARTIAL FULFILLMENT

OF THE REQUIREMENT FOR THE DEGREE OF

MASTER OF SCIENCE

in the department

of

Chemistry

SIMON FRASER UNIVERSITY

September 1978

Approval

Name : Septimus H. C. Liang

Degree : Master of Science

Title of Thesis : Investigation of Surface Acidic Sites on the Catalyst Silica-Alumina by C-13 Nuclear Magnetic Resonance Spectroscopy

Examining Committee :

Chairman : Dr. F. W. B. Einstein

Dr. Ian D. Gay
Senior Supervisor

Dr. E. J. Wells

Dr. A. C. Oehlschlager

Dr. D. Sutton

Date Approved September 6, 1978

Title of Thesis/Project/Extended Essay

Investigation of Surface Acidic Sites on the Catalyst Silice-Alumina by C-13 Nuclear Magnetic Resonance Spectroscopy

Author:

(signature)

Septimus Liang

(name)

January 24, 1979

(date)

Abstract

Developing a suitable probe gas is an essential step in the course of investigation of acidic sites on oxide surfaces. The problem at hand is complicated by the fact that silica-alumina is well known for its possession of both Bronsted and Lewis type acidic sites. The following experiments were initiated, first for the development of suitable probe gas, and then the final elucidation of total acidic sites and the Bronsted acidic sites concentration on this catalyst.

Carbon-13 NMR chemical shifts were measured for a series of alkyl pyridines, the corresponding alkylpyridinium ions and the adducts formed with boron trifluoride, and in some cases, with aluminum bromide.

The alkylpyridinium ions were formed by mixing the alkylpyridines with 10% excess 6M HCl, and with 1M tetramethylammonium chloride as internal standard. The chemical shifts were then corrected to TMS scale with appropriate susceptibility corrections.

The BF_3 and $AlBr_3$ adducts were formed by mixing the alkylpyridines (dried over molecular sieve type 4A) with 10% excess BF_3 or $AlBr_3$, using benzene as a solvent and an internal standard.

After a series of trials, 4-ethylpyridine seemed to be the best choice as a probe gas. Monolayers from 0.17 to 0.91 were obtained for 4-ethylpyridine chemisorbed on both water-treated and non-treated silica-alumina surface. The observed chemical shifts for C2 and C4 are appreciable. General resolution and signal to noise ratio from spectra are reasonable. We then relate the observed chemical shifts with the fractional protonated species , fractional coordinated species and the fractional physisorbed molecules, by means of two models.

Due to the limitations in our linear models, the exact concentration of both kinds of acidic sites could not be ascertained. Defects in the models were discussed with a proposed surface structure to correlate the findings.

To My Parents

Acknowledgements

If I have to buy beer for all those who helped me through this research project, I would go broke. So instead, I write this note to thank them all.

I am deeply indebted to Dr. Ian Gay for his most inspirational help in developing the thinking process in this thesis. I also like to thank Dr. A. K. Grover, Dr. Claude Lassigne and Mr. Steve Hensen for their sincere help and friendly discussions.

I would also like to thank Mr. Arthur Brooke, our NMR wizard, for his teachings and suggestions on how to use the XL-100 NMR machine. Mr. Peter Hatch's excellent glass-blowing and his teachings also helped me through this research project.

Last of all, I like to thank the Ginther's family for their enthusiasm, hospitality, help and providing a retreat where this thesis was done.

Table of Contents

List of Figures

List of Tables

Chapter I

I.1 Introduction

There are many definitions of acids and bases in the literature, notably those of Arrhenius (1), Franklin (2), Bronsted (3), Germann (4), Lewis (5), Ussanowitch (6), Bjerrum (7), Johnson (8), Lux, Flood et al., and Tomlinson (9), Shatenshtein (10), and Pearson (11). We may understand a solid acid in general terms as a solid on which the color of a basic indicator changes, or as a solid on which a base is chemically adsorbed. More strictly, following both the Bronsted and Lewis definitions, a solid acid shows a tendency to donate a proton or to accept an electron pair. This is possible with the presence of certain sites on the surface of the solid acid which can donate protons (protons are believed to be derived from attachment of water molecules on the surface)--- and known as Bronsted acidic sites, or electron-deficient sites (which accept electron(s) from the adsorbed molecules)---known as Lewis acidic sites. These definitions are adequate for an understanding of

the acid-base phenomena shown by various solids, and are convenient for the clear description of a solid acid catalyst as will be delivered in this thesis.

Solid acids have been found useful as catalysts for many important reactions including the cracking of hydrocarbons, the isomerization, polymerization and hydration of olefins, the alkylation of aromatics, and the dehydration of alcohols, etc.(12). Their importance in petroleum processing has stimulated a considerable amount of research into the adsorptive and acidic properties of solid surfaces. Among the most minutely studied acidic catalysts are natural clay minerals and mixed metal oxides, notably silica-alumina (SiO_2-Al_2O_3). Silica-alumina is well known for its strong acidity, possession of both Lewis and Bronsted acid sites, and uses as a catalyst for reactions like cracking of cumene (13), polymerization of ethylene oxide (14) and butene (15). It also has some significant oxidative properties (16). Yet little is known about the nature of acidic sites present on the surface of this catalyst.

In this work, concentration of surface acidic sites on silica-alumina will be elucidated by means of nuclear magnetic resonance study.

I.2 Statement of the Problem

From our previous study of adsorption of amines on various oxide surfaces (17), it has become essential to know the chemical shift changes of the amines upon protonation. The importance lies in the use of amines, such as N,N-diethylaniline in our case (17), as probe gases. If the acidic sites on the solid catalyst are of protonic type, then we would expect some of the adsorbed amine molecules to be protonated. The observed chemical shift changes would then reflect the total acid sites on the surface, if we assume that the protonated and non-protonated amine molecules exchange among themselves rapidly, thus the observed chemical shift is a weighted average of both. Chemical shifts of various free amines are available in literature (18,19,20,21), but not for their corresponding cations except pyridine and 4-methyl-pyridine (18,19). So our first task is to measure the

C-13 chemical shifts of a series of alkylpyridinium ions in aqueous HCl. Since previous results on free amines were obtained by continuous wave spectroscopy on a low frequency instrument, which is believed to be inaccurate, we have also re-measured the C-13 chemical shifts of this series of alkylpyridines. Together, we then obtain the net protonation shifts for the pyridine and alkylpyridines studied.

For further pursual of the problem, because of the existance of Lewis type sites on the surface of silica-alumina we have also measured the C-13 chemical shifts for the adducts formed by BF_3 with the alkylpyridines, and in some cases the $AlBr_3$ adducts. These results are then tabulated to permit the derivation of coordination shifts for the amines studied.

With the subsequent chemisorption of the probe gas (4-ethylpyridine in our case) on silica-alumina at various coverages and with or without water-treatment, we could measure the chemical shifts of the carbon atoms in the adsorbed 4-ethylpyridine. By comparison of these

chemical shifts with those of the 4-ethylpyridine in aqueous HCl and as a BF_3 adduct we may be able to derive the fraction of amines bonded to the Bronsted or Lewis sites, and thus a standard procedure could be obtained for the elucidation of the concentration of surface acidic sites (both Lewis and Bronsted) for all well studied surfaces.

Chapter II

II. Survey of Work Done on Silica-Alumina

Consider on a molecular scale the properties of the acid sites on a typical silica-alumina acidic catalyst. The following ideas have been generated through the years as a result of studying the interaction of "probe" gases with surfaces and consequently have given rise to the liquid phase concepts of Lewis and Bronsted acidity as applied to solids. In figure-1, we see the situation that might exist on a silica-alumina surface. The Al atom [1.a] requires an additional electron pair to complete its bonding. Thus, if the probe gas that interacts with this site has additional electrons that it can share with the aluminum atom, a chemical bond will form. This site is called a Lewis acid site.

Water molecules may be coordinated at the Lewis acid site to provide a source of protons [1.b]. This system is then regarded as a Bronsted acid. If the probe gas can accept the proton, and it forms, via electrostatic forces,

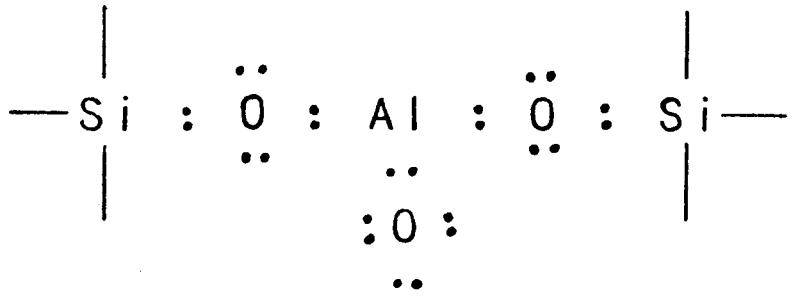

(a)

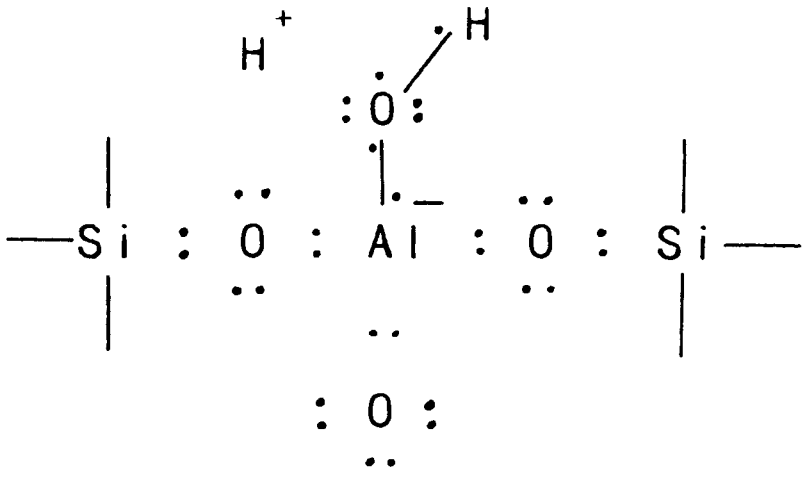

(b)

Figure 1 Simple electronic description of acid sites, (a) Lewis site; (b) Bronsted site.

a molecule bound to the surface, then there is a way of labelling this site. Certain probe gases have the ability to both donate electrons and accept protons. Pyridine is such a molecule (22).

Much controversy has been generated concerning the nature of the structure of silica-alumina. Numerous structures have been proposed, notably by Tamele (23), Hansford (24) and Planck (25). It is generally believed that the acid centres, whether of Lewis or Bronsted type, owe their existence in silica-alumina to an isomorphous substitution of trivalent Al atom for the tetravalent Si atom in the silica lattice. According to this view, a negative charge is created at this point on the solid surface [Fig.2.a]. Balancing this charge requires the detachment of an Al-O bond to restore the trivalency at the Al atom, thus creating a Lewis acid site [2.b]. Neutralization by the acquisition of a proton thus produces a Bronsted acidic site [2.c] in accordance with the configuration as depicted in Figure.1.

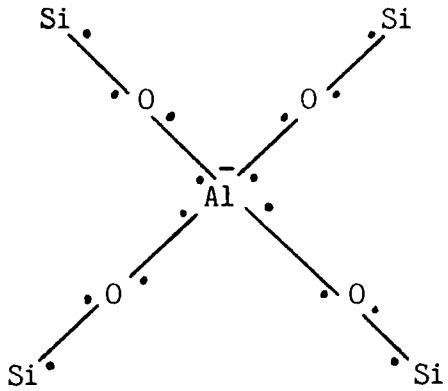

(a) Simple Surface Structure

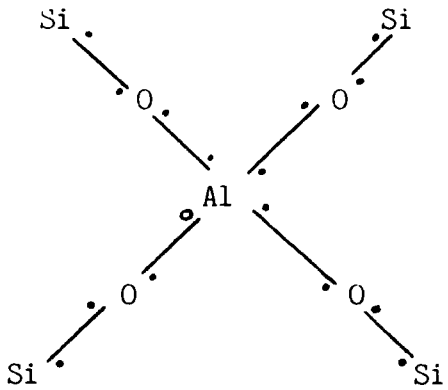

(b) Lewis Site with one electron hole

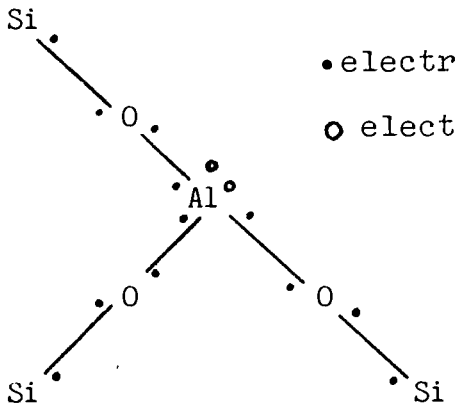

• electron

o electron hole

(b) Lewis Site with 2 electron holes

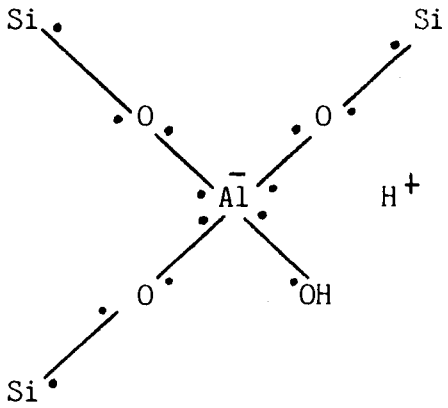

(c) Brosted Site

Figure 2 Various Aluminum Sites on the Silica-Alumina Surface

All studies indicate that silica-alumina has very strong acid sites, with strength H_o of at least -8.2, but the elucidated acidic sites concentration varies for different authors (12,26).

Recent studies of the infrared spectra of pyridine chemisorbed on synthetic silica-alumina have confirmed the presence of both Lewis and Bronsted acid sites (22, 28). The spectrum contains two main peaks, at 1540 cm^{-1} (discerned as the pyridinium ion); and at 1449 cm^{-1} (as strongly coordinated bound pyridine), and numerous other peaks discerned as physically adsorbed pyridines. After evacuation at 300 deg. C, the spectrum still indicates the presence of some pyridinium ions, but clearly shows the presence of Lewis acidity on the cracking catalyst, the lines at 1455 and 1459 cm^{-1} being quite marked. Upon addition of 0.05 mmole of water to the sample, an increase in the intensity of the 1540 cm^{-1} band indicates that a considerable amount of Bronsted acid has been formed, with a concomitant decrease in Lewis acidity at 1450 cm^{-1} . This conversion of Lewis sites to Bronsted

sites by water molecules has been confirmed by titration (29) and from studies of the infrared spectrum of adsorbed ammonia (30).

This later study consisted of a quantitative study of the ratio of Lewis to Bronsted acid sites on silica-alumina. The result revealed that the only detectable adsorbed species were physically adsorbed NH_3, ($P-NH_3$), coordinately bonded NH_3 ,($L-NH_3$) and NH_4^+. From the relative intensities of the appropriate bands, the ratio of $[NH_3]$ ($=[P-NH_3]+[L-NH_3]$) to $[NH_4^+]$ was found to be 4:1 at low concentration. The ratio decreases as concentration of adsorbed NH_3 increases.

However, infrared study of adsorbed molecules on a surface has its own drawbacks. The preparation of samples requires the oxide to be compressed into a wafer in the infrared cell, so that the amount of adsorbate is difficult to measure exactly. There are also the inherent difficulties in obtaining the extinction coefficients of the sample due to opaqueness. Finally, there is the associated uncertainty in the measurement of

peak intensity, thus the quantitative answers obtained (e.g. concentration of acidic sites) are not accurate.

Hall et al. (31) suggest on the basis of the deuterium exchange experiment and observation of the NMR spectra that the hydrogen on the surface of silica-alumina is chemically similar to that of alcohol, most of the hydrogen atoms existing in the form of SiOH, some of them as AlOH (with an upper limit on the number of Bronsted acid sites of 3×10^{13} H^+/cm^2) in good agreement with the infrared spectrum of adsorbed ammonia. Similar studies have been done by Schreiber and Vaughan (32) using NMR to measure the free induction decay constant (T_2) to assess the concentration of protons on the surface of silica-alumina with varying composition of silica. Both results are in reasonable agreement.

Chapter III

III.1 Nuclear Magnetic Resonance Studies of Adsorbed Molecules

Bloembergen, Purcell and Pound (BPP) (33) showed in 1948 that the nuclear magnetic resonance relaxation times are in certain cases intimately related to the motions of the molecule which contains the nuclei. The very next year, Spooner and Selwood (34) reported their applications of the BPP theory to the problem of catalysis, an important problem in surface chemistry. But it was not until 1956 when Zimmerman et al.(35) first reported their NMR studies of water adsorbed on silica gel that a continuing effort was begun to understand the implications of the BPP theory and its refinements for the motion of molecules adsorbed on surface.

III.2 Experimental Aspects of NMR Theory

This section is to describe in general terms, the approach to thermal equilibrium of a system of nuclear magnets in a constant magnetic field of strength H_o(36).

At equilibrium, the magnetization M_o of a system of nuclear spins $\hbar I$ with magnetic moments $\gamma \hbar I$ is given by Curie's Law :

[III.1] $M_o = N H_o \gamma^2 h^2 I(I+1)/(3kT)$

where $\hbar$ is Planck's constant over 2π, γ is the nuclear gyromagnetic ratio, k is the Boltzmann's constant and N is the number of nuclei in the system. The magnetic field exerts a torque upon the magnetic moments which gives the rate of change of the magnetization as:

[III.2] $d\vec{M}/dt = \gamma \vec{M} \times \vec{H}$

Now [III.2] contains no information about the approach to equilibrium, Bloch (37) accounted for these effects by introducing relaxation terms into [III.2], for $H_z = H_o$, $H_{xy} = 0$, his equations are :

[III.3] $dM_z/dt = -(M_z - M_o)/T_1$;

[III.4] $dM_x/dt = -M_y/T_2 + \gamma M_y H_o$;

[III.5] $dM_y/dt = -M_x/T_2 - \gamma M_x H_o$.

where T_1 is called the "longitudinal relaxation time" because it refers to relaxation along the field and T_2 is called the "transverse relaxation time" because it refers to relaxation transverse to H_o.

Another name for T_1 is the "spin-lattice relaxation time"; for longitudinal relaxation to occur the spin system must dissipate energy to the "lattice" or heat bath which is comprised of the remaining degrees of freedom (electronic, translational etc.) of the system. Likewise in certain cases T_2 may be called the "spin-spin relaxation time" because it refers to thermal equilibrium within the spin system itself.

It should also be noted that M_x and M_y can be measured experimentally as functions of time and that the relaxation behavior is therefore "knowable". Theory does not require, nor does experiment show that the longitudinal and transverse relaxation are always exponential.

Suppose the spin system, initially at thermal equilibrium is disturbed in such a way as to leave $M_x = M_o$ and $M_{y,z} = 0$ (as is often done in practice). The solution to [III.3] to [III.5] which gives the components of M at the time t after the disturbances are :

[III.6] $(M_o - M_z)/M_o = \exp(-t/T_1)$

[III.7] $M_x = M_o \cos(-\gamma H_o t)\exp(-t/T_2)$

[III.8] $M_y = M_o \sin(-\gamma H_o t)\exp(-t/T_2)$

while M_z relaxes exponentially to M_o, the transverse components make up a magnetic moment which rotates at a frequency of = H_o, the Larmour frequency, having an amplitude which decreases exponentially in time to zero. This rotating magnetic moment comprises the signal which can be observed with suitable apparatus. More elaborate derivations and discussions can be seen in ref.(38,39).

III.3 Magnetic Resonance Linewidths of the Adsorbed Species on the Surface

Magnetic resonance is useful in chemistry because nuclear magnetic resonance linewidths in liquids are so narrow that resonance frequencies differing by as little as a part in 10^8 may often be resolved. Since NMR phenomena are determined by molecular kinetics and structural parameters, NMR pulse experiments can be used to study motional phenomena of adsorbed molecules.

Relative motions or fluctuating dipole-interactions of adsorbed molecules with a magnetic surface generally determine the line shape and width of the NMR resonance line. We could imagine chemisorbed molecules being held to the surface by forces greater than Van der Waal's force in magnitude. These forces would then decide the motions of the molecules on the surface. If the sorbed molecules are only loosely bound to the surface, they would have rapid motions and thus a narrower linewidth than a system of more tightly bound molecules. Notice that a rise in temperature can also induce rapid motions in the sorbed molecules even if they are tightly bonded. Static dipole-dipole interactions may also cause the broadening of NMR resonance lines. Thus T_2, the transverse relaxation time, which is a direct result of the interactions between two magnetic dipoles, is usually taken as a measure of the linewidth of the resonance lines in the absence of chemical shift broadening. Use of powdered samples, which reduces the magnetic field inhomogenity also results in narrower linewidth (40).

III.4 Relaxation Mechanisms of Adsorbed Molecules on Surfaces

The relaxation of adsorbed molecules has thus far been studied with both the conventional NMR apparatus and the spin-echo systems, so that no specific discussion is required here. Detailed reviews can be seen in ref.(40,41,42,43). What is described here is a simple mechanism by which adsorbed molecules could relax.

One expects several changes in the relaxation mechanisms of molecules after they become adsorbed on a surface. Molecules which formerly rotated isotropically may now be expected to have a preferential axis of rotation. If the molecule in the bulk phase relaxed through some intermolecular dipole-dipole mechanisms, then one would expect this to be severely altered on a surface, the relaxation in this case becoming coverage dependent. One would expect relaxation to be caused by dipole-dipole interactions with magnetic dipoles associated with the surface, as for example, with the hydroxyls on an oxide surface. Obviously, a surface could enhance relaxation if it contains paramagnetic species.

When analyzing C-13 spin-lattice relaxation in liquids, one must consider three possible relaxation mechanisms (39,43), namely chemical shift anisotropy ("csa"), spin rotation interactions ("sr") and the C-H dipole-dipole interactions ("d-d"). The last one is expected to be predominant for protonated carbons, except in very small molecules (44), while chemical shift anisotropy may be an important relaxation mechanism for some non-protonated carbons, especially at high resonance frequencies (45). As an additional contribution to the C-13 relaxation rate of adsorbed molecules, the magnetic coupling of carbon nuclei with paramagnetic ions ("ions") is to be taken into account (43,46). Thus T_1, the spin-lattice relaxation time constant, is given by

$$[III.9]\quad T_1^{-1} = T_1^{-1}(csa) + T_1^{-1}(sr) + T_1^{-1}(ions) + T_1^{-1}(d\text{-}d)$$

The relaxation rate $T_1(d\text{-}d)$ is easy to analyze. Because long range C-H interactions can be neglected, only the coupling with protons attached to the individual carbon has to be taken into account . Denoting the bond

length between carbon and hydrogen by r_{CH}, the correlation time of thermal motion by τ_c, and assuming in this discussion only $T_1(d\text{-}d)$ is the important contribution to T_1 i.e. $T_1 \simeq T_1(d\text{-}d)$, we obtain for a CH_n group, with the narrowing limit of $(\omega\tau_c)^2 << 1$,

[III.10] $$T_1^{-1} = n \gamma_C^2 \gamma_H^2 \hbar r_{CH}^{-6} \tau_c$$

Therefore for a typical T_1 value in the 0.2 to 1 sec. range (47), τ_c will be of the order $\sim 10^{-11}$ sec. This would imply thermal motion mainly of translational jumps and rotational jumps among the sites on the surface.

This is only a lower estimate of τ_c. For molecules chemisorbed on surfaces, we would expect the motions to be hindered and a higher range of τ_c values according to the following relationship (46) for a CH_n group

[III.11] $$T_1^{-1} = \frac{1}{15} \gamma_C^2 \gamma_H^2 I(I+1) r_{CH}^{-6} n \hbar^2 \left[\frac{6\tau_c}{1+\omega_C^2\tau_c^2} + \frac{12\tau_c}{1+(\omega_C+\omega_H)^2\tau_c^2} + \frac{2\tau_c}{1+(\omega_C-\omega_H)^2\tau_c^2} \right]$$

In general, T_1 for a dipolar relaxation of unlike spins is given by (39) as

[III.12] $$T_1^{-1} = \hbar \gamma_I^2 \gamma_S^2 \, I(I+1) \left[\frac{1}{12} J^{(0)}(\omega_I - \omega_S) + \frac{3}{4} J^{(2)}(\omega_I + \omega_S) \right]$$

where I and S denote different spins and $J^{(q)}(\omega)$ is the spectral density function of the form

$$\tau_c \Big/ \left[1 + (\omega \tau_c)^2 \right]$$

where τ_c is again, the correlation time.

Quantitative evaluations of other contributions are not as easy. The relaxation mechanism of next importance is the coupling with the paramagnetic ions (usually existing as impurities on the oxide surface), the evaluation consists not only of the concentrations and distributions of the paramagnetic impurities but also the electron spin of the species which is generally unknown (48).

T_2, the spin-spin relaxation time, which is equal approximately to the reciprocal of linewidth at half intensity, is given by (39) as

[III.13] $$T_2^{-1} = \hbar \gamma_I^2 \gamma_S^2 \, S(S+1) \left[\frac{1}{6} J^{(0)}(0) + \frac{1}{24} J^{(0)}(\omega_I - \omega_S) + \frac{3}{4} J^{(1)}(\omega_I) + \frac{3}{2} J^{(1)}(\omega_S) + \frac{3}{8} J^{(2)}(\omega_I + \omega_S) \right]$$

The constants in front of the bracket can be written as $k_d M_2$ where k_d is a constant characteristic of the type of motion in consideration i.e. translation or rotation, and M_2 is the Van Vleck second moment (49). In the case of $(\omega\tau_c)^2 << 1$, [III.13] can be approximated the same way as [III.10] i.e.

[III.14] $T_2^{-1} \cong \tau_c M_2$

For a typical linewidth of 100 Hz (which is usual in our case as shown later in typical spectra of the adsorbed molecules) and M_2 of the order of 10^8 Hz^2. τ_c is of the order of 10^{-6} second.

Thus molecular motions are fast enough to average out the C-H dipolar linewidths to a few hundred Hz in our spectra, and we are able to observe chemical shifts of the carbon atoms on the probe gases, when adsorbed on the surface.

The criteria by which carbon-13 was selected for this study, as opposed to other nuclei, e.g. proton, should be noted. From the above estimation, since the

gyromagnetic ratio of C-13 is small , so that there is a weak coupling to the protons on the same molecule and to the paramagnetic impurities on the surface, thus narrow linewidths would be observed. The proton spectra on the other hand would be expected to be broad due to the strong H-H dipole-dipole interactions and also the interactions with surface paramagnetic impurities due to the large gyromagnetic ratio of both. And indeed, this is the result in our present study. The proton spectrum of 4-ethylpyridine on silica-alumina consists of two broad, featureless resonances about 500 Hz wide, but the C-13 spectrum for the same system consists of five resonances each about 40-100 Hz wide (Figure 3). Thus one is able to assign all five resonances to the five different carbons in the molecule. Also due to the larger chemical shift changes observed for C-13 from the above spectrum , we can conclude that C-13 spectra of the adsorbed system are more informative, in agreement with previous results (46).

Paramagnetic species present on the surface may cause some problems in the resolution of the spectra of adsorbed molecules. Assuming Fe^{3+} ions are the only paramagnetic impurity in our sample, and that they are evenly distributed on the surface, we can estimate their effect on the linewidth of the resonance lines. For our sample, the concentration of Fe_2O_3 is 0.05% (wt.), therefore the ratio of number of Fe atoms to number of Al atoms is about 1.3×10^{-3}. Assuming on the surface of silica-alumina, the oxygen atoms are hexagonally close-packed with Si and Al atoms filling the tetrahedral sites, according to their ratio, this will then give 2.3×10^{14} Al atoms per sq.cm. Correspondingly, this will give 2.9×10^{11} Fe^{3+}/sq.cm., or an average distance of about 200 A between Fe^{3+} ions. If we further assume that the adsorbed amines are situated among these Fe^{3+} ions, that is, distributed evenly upon adsorption, then the average distance between the carbon atoms of the amine and these Fe^{3+} ions is about 100 A. Noting that the ratio of magnetic moment of Fe^{3+} to proton is about 5700 times, we can then estimate the difference of dipole interactions of carbon to Fe^{3+} (D_{Fe}) and

of carbon to proton (D_H) with an average distance of about 1.1 A. The ratio of D_{Fe} to D_H would be given as $5700x(r_{CH}/r_{C-Fe})^3 = 7.6x10^{-3}$. If the correlation times for both dipole relaxations are the same, then we would expect the line broadening by proton to be about 130 times more important than the line broadening by the Fe^{3+} ions.

Caption

Figure 3.A. Proton Spectrum of 4-ethyl-pyridine on silica-alumina at 0.53 monolayer, run at 28 deg C. 100 scans.

Figure 3.B. Carbon-13 Spectrum of the same sample, run at 80 deg C. 15,000 scans.

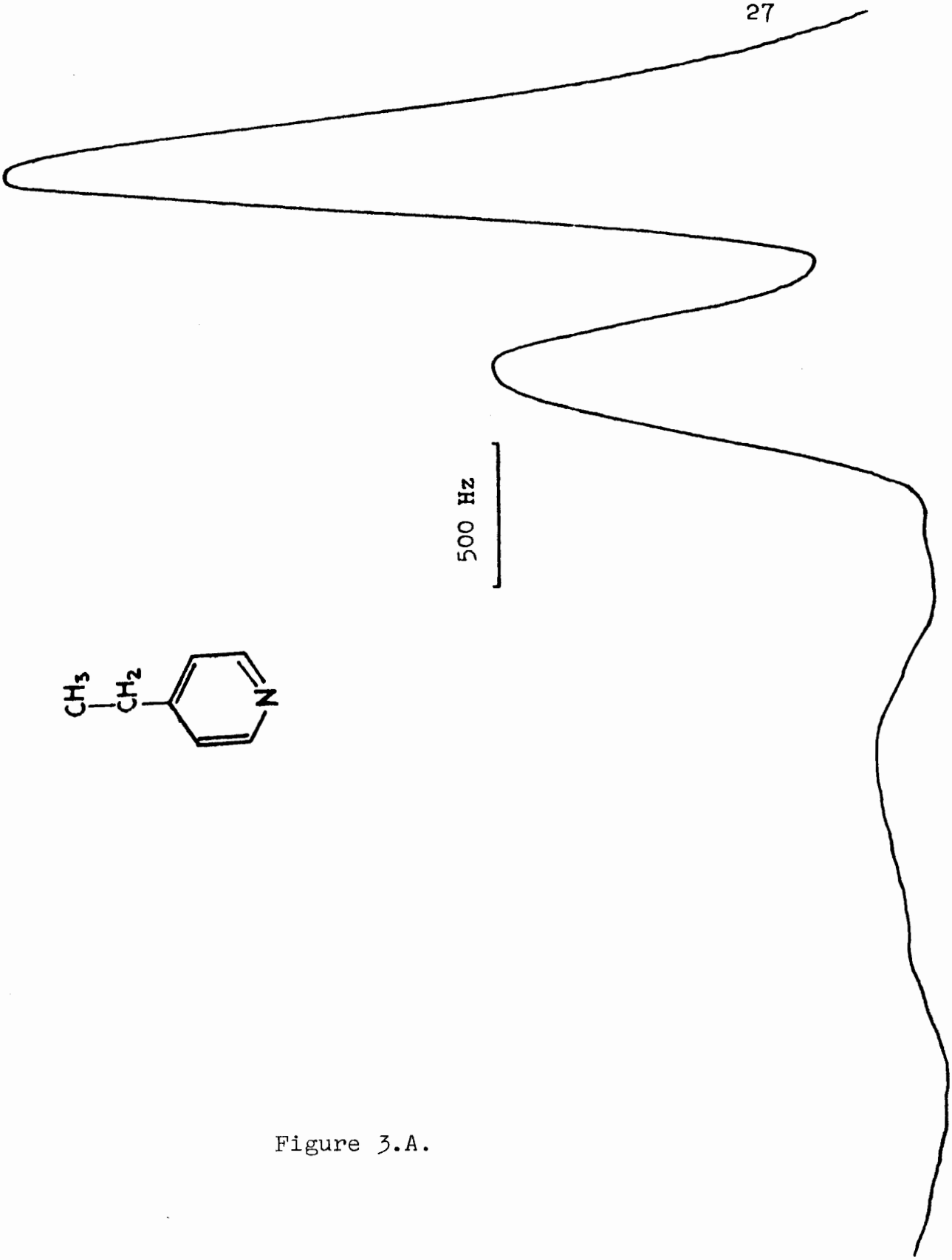

Figure 3.A.

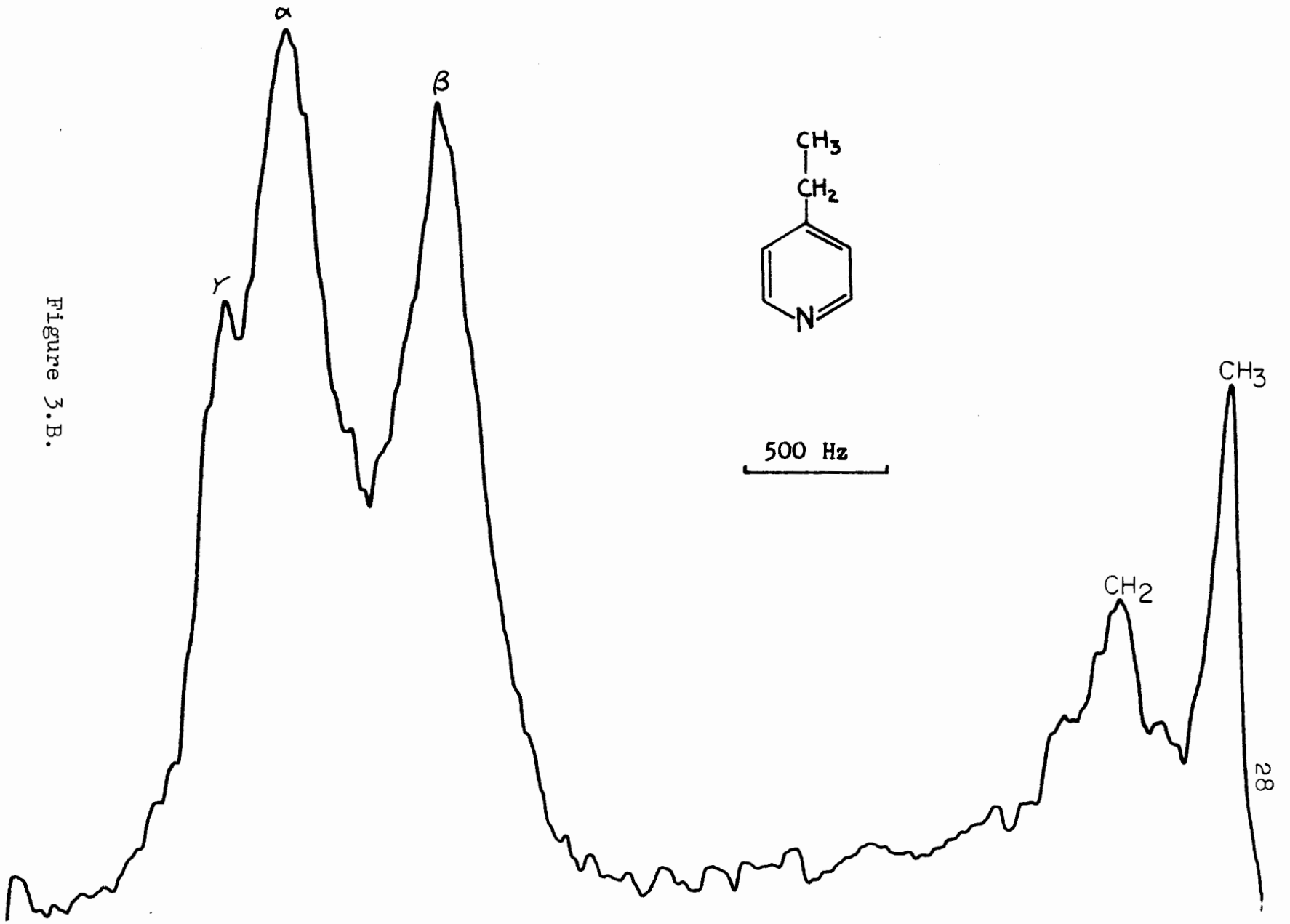

Figure 3.B.

Chapter IV

Experimental

IV.1 Apparatus

Nuclear magnetic resonance studies were performed on a Varian Model XL-100 spectrometer operating at a magnetic field of 23.5 kilogauss and an RF frequency of 25.16 MHz for carbon-13. The field is modulated at a fixed frequency of 40.96 KHz permitting the use of an external fluorine-19 CW lock. It is also equipped with a pulsed internal deuterium lock for adjusting homogenity of magnetic field. The probe unit is a standard Varian Model V-4412 with insert for 12 mm sample tubes. The spectrometer is also equipped with a single sideband accessory. A proton-noise decoupling system operating at 100 MHz is also used in conducting experiments. A Nicolet 1080 computer is built on-line to the spectrometer for the pulsed-Fourier transform operations utilizing a TT-100 accessory. Pulse control and acquisition of data is done with a Nicolet Model 293 pulse timer and a 294 disk accessory.

All NMR experiments were performed at 25.16 MHz on this Varian XL-100 spectrometer. Proton noise decoupling was used in all experiments, except when off-resonance coherent decoupling was required for assignments. The external fluorine-19 lock was used throughout all experiments. Normally an 18 sec. (approx. /3) pulse was used at a repetition rate of one per ten seconds, on an 8K memory allocation, to obtain the chemical shifts of the free amines and their corresponding cations and adducts formed with BF_3 and $AlBr_3$.

For the silica-alumina samples, a repetition rate of five per second was used. Between 10^5 and $1.4x10^6$ scans were taken for each spectrum depending on the concentration and linewidth, on a 2K memory.

Proton spectra were run for some samples to investigate the possibility of utilizing proton NMR in surface study. These experiments were performed at 100 MHz on the same XL-100 machine with a 5 sec pulse at a repetition rate of five per second. A typical spectrum was shown in Figure.3.A.

All spectra were run at approximately 28 degrees celsius, unless otherwise stated.

IV.2 Silica-Alumina Samples

The sample of silica-alumina used is a Grade-980, 25 wt.% alumina product from Davison (Grace) Company, in the form of 3/16"x3/16" cylindrical pellets with a bulk density of 39 lb/cu.ft. and a surface area of 400 sq.m. per gm. The pore volume is 0.70 cc/gm with an average pore diameter of 70 A. This sample was calcined at 500 degree C for 24 hours and then ground to 20-40 mesh powder before storing in 100 % relative humidity. The surface area of this silica-alumina was determined to be 333 sq.m./gm. by the BET method using nitrogen. The main impurities in this oxide consist of 0.05% Fe_2O_3 and 0.04% Na_2O, from manufacturer's analysis.

IV.3 Reagents

The pyridine and alkylpyridines for the measurement of protonation and coordination shifts were from various commercial sources. Prior to use, they were distilled

at reduced pressure and then stored over molecular sieve type 4A. The hydrochloric acid used was diluted with deionized water from concentrated hydrochloric acid produced by Mallinckrodt Chemical Co. The tetramethylammonium chloride was produced by Eastman Kodak Co. The boron trifluoride was obtained in lecture gas-cylinder from Matheson Co. The $AlBr_3$ used was from Fisher Scientific Co.

IV.4 Preparation of Protonated Pyridines and Alkylpyridines and Their NMR Measurements

C-13 NMR spectra of the amines were recorded for samples of the neat pyridines with 10% (vol.) tetramethylsilane (TMS) added as an internal reference. The cation samples were prepared by adding the amine to 6M HCl so that 10% of the acid remained in excess. 1M tetramethylammonium chloride (TMACl) was added as an internal reference. For the case of pyridinium ion, a concentric 5 mm. tube containing TMS was put into the solution, so that the chemical shifts of TMACl relative to TMS could be measured. The measured shift

is 56.68 ppm which is in good agreement with the literature value of 56.54 ppm reported by Sarneski et al.(50). Assuming that this value does not change from one amine to another, we obtained the cation shift of the series of alkylpyridinium ions with respect to TMS, with the appropriate susceptibility corrections. These results were then combined with the chemical shifts of the neat amines to give the protonation shifts for all species.

The assignments of the various resonances on the NMR spectra were done in several ways. For the previously reported amines, we assume the assignments in literature (18,19) to be correct. However, for the protonated species, only pyridinium and 4-methylpyridinium ions are reported (18), therefore separate assignments were necessary. For the more symmetrical species, this can be done from intensity ratios, off-resonance decoupling and the broadening of the C2 and C6 resonances which results from coupling to the N-14 quadrupolar nucleus. In the case of 2-methylpyridine and 3-methylpyridine, the above information is not enough.

We prepared the HCl-amine solutions of different compositions; due to the fast exchange, only a single resonance is observed for each carbon in the solution and we were able to observe a continuous transition from the line position of the neat amine to that of cation species, as excess acid is added. These experiments establish the relationship between cation and neat amine resonances, and enable one to assign the cation shifts. There was no literature value for 4-n-propylpyridine, but observing that the methyl and methylene resonances in 4-ethylpyridine are close to those of ethylbenzene (51), we assume that the same analogy would exist for the n-propyl compounds. We therefore assign the lower field methylene resonance to the carbon to the ring.

IV.5 Preparation of BF_3 Adducts with Pyridine and Alkylpyridines and Their NMR Measurements

Purified amines were dissolved in benzene (Fisher Scientific analytical grade) (v/v:1/6) and degassed inside a 12 mm (o.d.) pyrex tube. Boron trifluoride was

then introduced into the benzene solution by the conventional gas-volumetric method to ensure a 10% excess of boron trifluoride.

C-13 chemical shifts were measured for both the neat pyridine and alkylpyridines in benzene and for the BF_3 adducts, with respect to benzene. The assignments of chemical shifts for the adducts are quite similar to those previously discussed. A special case arose for the adduct formed by 2-methylpyridine. Apparantly the C3 resonance was 'hidden' by the benzene peak, therefore chloroform was used as a solvent and all resonances were clearly assigned.

The pyridines-$AlBr_3$ complexes were prepared the same way. The $AlBr_3$ used was first sublimed and then added to the benzene solution containing the pyridine or alkylpyridines. The preparation was carried out under nitrogen inside a dry box to ensure that the complex would not be hydrolysed. The solution containing the complex was then transfered to a 12 mm NMR tube and degassed.

IV.6 Preparation of Adsorbate- Silica-Alumina Samples for NMR Measurements

Most of these amines do not have an appreciable vapor pressure at room temperature, so the preparation of samples requires a special apparatus (Figure 4). The oxide for NMR measurement was contained in 12 mm (o.d.) pyrex tubes, which were then glass-blown to A. After degassing procedure, the stopcock to A was closed. Measured amounts of adsorbates were put into compartment B which was then degassed. The two compartments were then brought into communication by opening all stopcocks except C and were then equilibrated in an oven at 90°C for at least an hour and then allowed to cool. In no case was any liquid amine visible after this treatment, and since the amount of gas phase amine would be negligible, at the vapor pressure of the liquid, we could assume that essentially all of the amines were adsorbed on the solid sample. Water-treated samples were prepared by the same technique, a measured amount of water being added to the same compartment as the amine. Average deviation in the measurement of transferred amines is ± 0.05 moles/sq.m.

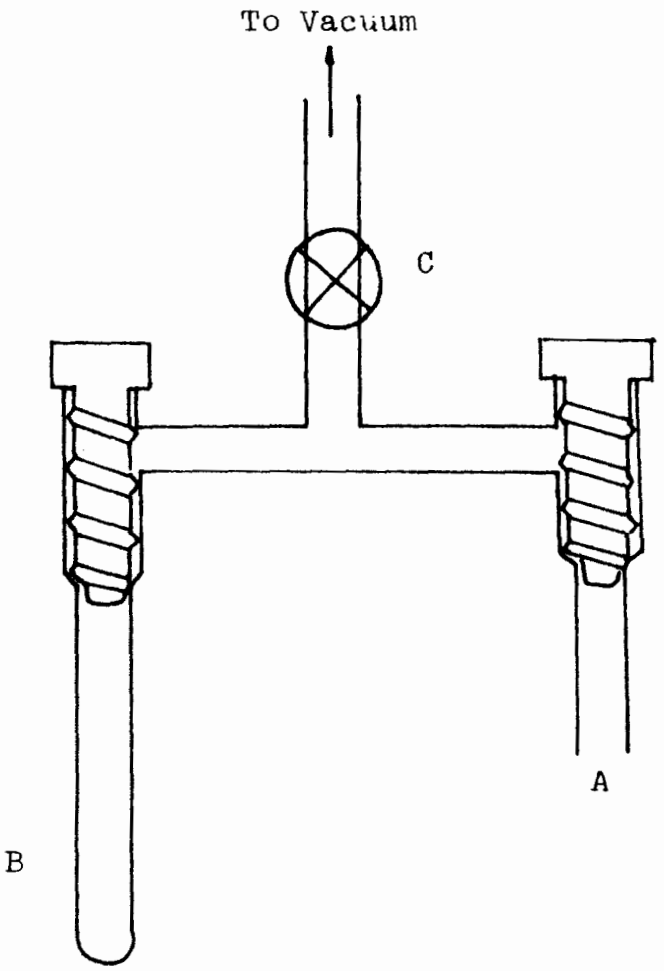

All stopcocks are teflon-type with silicone seal from Ace Glass Co. Compartment B has a volume of about 0.5 ml.

Figure 4

Apparatus for the preparation of samples.

Chemical shifts were measured relative to external samples of the neat liquid amines, using a susceptibility correction determined from proton spectroscopy of phsically adsorbed TMS (52), of 0.4 ppm downfield.

Spectra were run at temperatures ranging from ambient (approx. 28°C) to 80°C. In general, narrower lines could be achieved at higher temperatures. But too high a temperature resulted in distillation of adsorbate to the cooler regions of the sample tube. The measurement was always at least twenty degrees below the temperature at which visible liquid condensate appeared on the cool regions of the sample tube.

A special sample was prepared for 4-ethylpyridine on pure silica gel at 0.91 monolayer. The silica gel was a Davison Grade 923 product with a surface area of 560 sq.m. per gm. and an impurity of 0.05% Fe_2O_3. The NMR spectrum was obtained in the same way as for other samples. This experiment was designed to measure the chemical shifts of physically adsorbed 4-ethylpyridine. This assumption is valid since silica gel is believed

to be inert and its interaction with weak base is not stronger than hydrogen bonding (15,17,53), which is applicable in our case in defining the physically sorbed 4-ethylpyridine on silica-alumina, because of the low fraction of Al atoms in the surface structure. The observed chemical shift for C2 is - 0.9 ppm and 1.5 ppm for C4 after susceptibility correction (52).

Chapter V

Results and Interpretation

V.1 The Protonation Shifts of Some Alkylpyridines

Results of this experiment are tabulated in Table 1, together with the susceptibility corrected cation shifts and net protonation shifts.

The necessary susceptibility correction is 0.4 ppm downfield. So although our data are measured up to ±0.03 ppm from the digital resolution, we have to report the data to ±0.1 ppm, due to uncertainties in calculating this correction.

Our measured chemical shifts for neat pyridines are in good agreement with the literature values (17,18,19, 20). Slight variance exists for the alkylpyridines when compared to those of Lauterbur (20) and then converted to the TMS scale by Stothers (51). Our measurements are constantly one ppm more upfield than his, except for

4-ethylpyridine. This difference may be due to systematic error in his experiment, or in the necessary conversion to the TMS scale.

Our observed pyridinium ion chemical shifts lie somewhat between that of Pugmire and Grant (18) and Lavallee et al.(19). This again may be due to systematic errors since the older experiments were done by continuous wave spectroscopy on a low frequency NMR spectrometer, which is thought to be inaccurate. Also, there may be some mistake in Lavallee's data, since methanol was used as an internal standard and assumed not to be affected by the H^+ or H_2O present.

Effects of methyl substitution on ring carbons are additive as pointed out by Lauterbur (20). This is confirmed by our result of chemical shifts of neat pyridines and alkylpyridines, as shown in Table 2. Thus the ring carbons shifts of poly-methylpyridines can be predicted to $\pm$ 0.2 ppm, by comparing the data for pyridine and monomethylpyridines.

Unfortunately, the additive property is not observed for the methylation , nor for the protonation shifts of the alkylpyridinium ions. Thus if one determines methylation effects by comparing the pyridinium and monomethylpyridinium ions, these figures fail to reproduce the C4 shifts of 2,6-dimethylpyridinium by 7 ppm and the C2 shift of 2,4,6-trimethylpyridinium ion by 6 ppm.

From the observation of the data, substitution at C2 tends to decrease the C2 protonation shift, and substitution at C4 tends to increase the C4 protonation shift. The methyl groups only have an appreciable shift when substituted at C2 and it is upfield in all cases.

The upfield protonation shift for C2 on pyridinium ion is explained by Pugmire and Grant (18) as arising from the decrease in N-C bond order upon protonation. Thus, protonation serves to deshield the β and γ carbons substantially while increasing the shielding at the α position. With a methyl substitution at C2, there will be a σ donation from the methyl group, with a subsequent decrease in the $C\text{-}CH_3$ order. This could then produce the upfield shifts for C2 and the methyl groups as observed.

This explanation may be oversimplified. Recent molecular orbital calculations on N-15 chemical shifts (54) reveal the same upfield shift for nitrogen from pyridine to pyridinium ion. Their explanation is that there is a change in excitation energy basing on the evaluation of paramagnetic component of the screening tensor. This argument may be applied to C2 and other nuclei of the pyridinium ion to explain the "wrong" way that the chemical shifts go.

Table 1

C-13 Chemical Shifts of Pyridine and Alkyl-Pyridines and Their Corresponding Cations (ppm)

Amine and C-Atoms	Free Amine Shifts wrt TMS	Raw Cation Shifts wrt TMACl	Corrected Cation Shifts wrt TMS	Protonation Shifts (±0.1 ppm)
Pyridine				
2	150.26	85.77	141.9	-8.3
3	123.96	72.17	128.3	4.4
4	135.90	91.77	147.9	12.0
2-methylpyridine				
2	158.60	98.18	154.3	-4.3
3	123.17	72.71	128.9	5.7
4	135.99	91.14	147.3	11.3
5	120.80	69.12	125.3	4.5
6	149.51	84.90	141.1	-8.5
CH_3	24.48	-35.92	20.2	-4.2

Amine and C-Atoms	Free Amine Shifts wrt TMS	Raw Cation Shifts wrt TMACl	Corrected Cation Shifts wrt TMS	Protonation Shifts (±0.1 ppm)
3-methylpyridine				
2	150.71	85.15	141.3	-9.4
3	133.15	83.44	139.6	6.5
4	136.21	92.18	148.3	12.1
5	123.30	71.48	127.6	4.3
6	147.33	82.86	139.0	-8.3
CH_3	18.14	-37.37	18.8	0.7
4-methylpyridine				
2	150.02	84.69	140.9	-9.2
3	124.81	72.57	128.7	3.9
4	146.74	105.90	162.1	15.3
CH_3	20.60	-33.28	22.9	2.3
4-ethylpyridine				
2	150.17	84.96	141.1	-9.1
3	123.48	71.37	127.5	4.1
4	152.58	110.93	167.1	14.5
CH_2	28.27	-26.58	29.6	1.3
CH_3	14.45	-42.24	13.9	-0.5

Amine and C-Atoms	Free Amine Shifts wrt TMS	Raw Cation Shifts wrt TMACl	Corrected Cation Shifts wrt TMS	Protonation Shifts (±0.1 ppm)
4-n-propylpyridine				
2	150.08	84.90	141.1	-9.0
3	124.02	71.94	128.1	4.0
4	150.98	109.65	165.8	14.8
αCH_2	37.30	-18.03	38.1	0.8
βCH_2	23.75	-32.84	23.3	-0.4
CH_3	13.74	-42.30	13.9	0.1
4-t-butylpyridine				
2	149.93	84.95	141.1	-8.8
3	120.48	68.98	125.1	4.7
4	158.99	117.08	173.2	14.3
$-\overset{\vert}{\underset{\vert}{C}}-$	34.35	-19.37	36.8	2.4
CH_3	30.39	-26.09	30.1	-0.3
2,6-dimethylpyridine				
2	157.71	90.62	146.8	-10.9
3	119.90	69.46	125.6	5.7
4	136.20	97.55	153.7	17.5
CH_3	24.45	-36.22	19.9	-4.5

Amine and C-Atoms	Free Amine Shifts wrt TMS	Raw Cation Shifts wrt TMACl	Corrected Cation Shifts wrt TMS	Protionation Shifts (± 0.1 ppm)
3,5-dimethylpyridine				
2	147.86	82.74	138.9	-9.0
3	132.37	82.35	138.5	6.1
4	136.71	92.35	148.5	11.8
CH_3	17.99	-37.58	18.6	-0.6
2,4,6-trimethylpyridine				
2	157.49	96.35	152.5	-5.0
3	120.81	69.90	126.1	5.3
4	146.67	104.49	160.7	14.0
CH_3(2,6)	24.28	-36.55	19.6	-4.7
CH_3(4)	20.56	-33.79	22.4	1.8

Note : The protonation shifts are obtained from difference of free amines and the cation shifts. Minus sign indicates an upfield shift.

See text for estimate of uncertainties.

Table 2

The Effects of Methyl Substitution on Ring C-13 Magnetic Shieldings in Pyridines (in ppm)

Methyl Position	Ring Carbon Positions 2	3	4	Methyl Derivatives
		Ortho Effect		
2	-----	- 0.8	-----	2-methylpyridine
2	-----	- 1.0	-----	2,6-dimethylpyridine
3	+ 0.5	-----	+ 0.3	3-methylpyridine
3	+ 0.6	-----	+ 0.5	3,5-dimethylpyridine
4	-----	+ 0.9	-----	4-methylpyridine
4	-----	+ 1.0	-----	2,4,6-trimethylpyridine
		Meta Effect		
2	- 0.8	-----	+ 0.1	2-methylpyridine
2	- 0.9	-----	+ 0.2	2,6-dimethylpyridine
3	-----	- 0.7	-----	3-methylpyridine
3	-----	- 0.8	-----	3,5-dimethylpyridine
4	- 0.2	-----	-----	4-methylpyridine
4	- 0.3	-----	-----	2,4,6-trimethylpyridine

Methyl Position	Ring Carbon Positions 2	3	4	Methyl Derivatives
		Para Effect		
2	-----	- 3.1	-----	2-methylpyridine
2	-----	- 3.3	-----	2,6-dimethylpyridine
3	- 3.0	-----	-----	3-methylpyridine
3	- 2.8	-----	-----	3,5-dimethylpyridine
		Direct Substitution Effect		
2	+ 8.4	-----	-----	2-methylpyridine
2	+ 8.3	-----	-----	2,6-dimethylpyridine
3	-----	+ 9.2	-----	3-methylpyridine
3	-----	+ 9.1	-----	3,5-dimethylpyridine
4	-----	-----	+10.8	4-methylpyridine
4	-----	-----	+10.4	2,4,6-trimethylpyridine

Note: sign notations same as in Table.1.

V.2 The Coordination Shifts of Some Alkylpyridines

Results of this experiment are collected in Table 3, together with the adduct shifts and the net coordination shifts. Adduct shifts formed with $AlBr_3$ are collected in Table 3A, for pyridine, 2,6-dimethylpyridine and 4-ethylpyridine. The observed chemical shifts were then converted to the TMS scale from the 128.49 ppm we observed for benzene downfield from TMS.

The associated uncertainty in the reported data is $\pm$0.03 ppm. It is different from that of the protonated case, because benzene is used as internal reference and no susceptibility correction is required.

There is slight variance between the chemical shifts of the adducts formed with BF_3 and $AlBr_3$. Basically, it is due to the fact that bromide is a bulky group, so it will lessen the strength of the bond formed between aluminum and nitrogen. Thus this steric hindrance will induce a charge on nitrogen that is less positive than that would be formed from BF_3 and thus a stronger bond

order in the N-C bond with the result of a smaller upfield shift for C2 on pyridine and 2,6-dimethylpyridine, which, in this case, even the σ donation from the methyl group will not have much effect on the C2 shift. It is interesting to note that the magnitude of C4 shift is higher in the $AlBr_3$ adducts than those of the BF_3 adducts. Apparently, C4 is more deshielded in the former compound due to the same argument given above.

As could be observed, the upfield C2 coordination shift is smaller than the corresponding protonation shift for the 2-substituted alkylpyridines, by 2.1 ppm for 2-methylpyridine, 11 ppm for 2,6-dimethylpyridine and 4.3 ppm for 2,4,6-trimethylpyridine. The explanation is that, for the cation species, we have a full positive charge at the nitrogen atom, while only a partial positive charge for the adducts. Thus the decrease in N-C bond order is bigger in the case of cation species, and therefore the observation.

While this electrostatic reasoning may contribute to the total effect, the mechanism for the C-13 shift given earlier for the protonation shift may still apply in this case, that is, the change in paramagnetic contribution in the screening tensor may still be dominant.

In general, the trend that is observed in the protonated species still applies to the adduct species, e.g. the decrease in the C2 shift as methyl group is substituted there. As could be seen in Table 4, the additive properties of methyl substitution is not observed also for the BF_3 adducts.

Table 3

C-13 Chemical Shifts of the BF_3 Adducts formed with Pyridine and Its Alkyl Derivatives.

Amine and C-atoms	Free Amine Shift wrt TMS (ppm)	BF_3 Adduct Shift wrt TMS (ppm)	Coordination Shift (ppm)
Pyridine			
2	150.17	142.94	- 7.23
3	123.54	126.00	2.46
4	135.34	142.80	7.46
2-methylpyridine			
2	158.56	156.42	- 2.14
3	122.90	128.51	5.61
4	135.61	142.55	6.94
5	120.52	122.88	2.35
6	149.49	143.51	- 5.98
CH_3	24.46	20.91	- 3.55

Amine and C-Atoms	Free Amine Shift wrt TMS (ppm)	BF_3 Adduct Shift wrt TMS (ppm)	Coordination Shifts (ppm)
3-methylpyridine			
2	150.71	143.38	- 7.33
3	132.86	136.96	4.10
4	135.86	140.10	4.24
5	123.01	125.47	2.46
6	147.32	142.96	- 4.36
CH_3	17.97	17.62	- 0.35
4-methylpyridine			
2	150.14	142.14	- 7.89
3	124.51	126.61	2.10
4	146.24	156.36	10.12
CH_3	20.49	20.89	0.40
4-ethylpyridine			
2	150.14	142.14	- 7.89
3	123.22	125.32	2.10
4	152.18	161.64	9.46
CH_2	28.10	28.22	0.12
CH_3	14.27	13.12	- 1.15

Amine and C-Atoms	Free Amine Shift wrt TMS (ppm)	BF_3 Adduct Shift wrt TMS (ppm)	Coordination Shifts (ppm)
4-n-propylpyridine			
2	150.12	142.50	- 7.62
3	123.82	125.82	2.00
4	151.13	160.30	9.17
αCH_2	37.14	37.04	- 0.10
βCH_2	23.51	22.72	- 0.79
CH_3	13.64	13.36	- 0.28
4-t-butylpyridine			
2	150.23	142.75	- 7.48
3	120.56	121.73	1.17
4	159.02	168.27	9.25
$-\overset{\vert}{\underset{\vert}{C}}-$	34.28	30.29	- 3.99
CH_3	30.36	29.59	- 0.77
2,6-dimethylpyridine			
2	157.82	157.90	+ 0.08
3	119.83	126.16	6.33
4	136.07	141.08	5.01
CH_3	24.41	23.58	- 0.83

Amine and C-Atoms	Free Amine Shift wrt TMS (ppm)	BF_3 Adduct Shift wrt TMS (ppm)	Coordination Shifts (ppm)
3,5-dimethylpyridine			
2	147.90	140.41	- 7.49
3	132.19	136.08	3.89
4	136.58	143.57	6.99
CH_3	17.86	18.47	0.49
2,4,6-trimethylpyridine			
2	157.59	156.92	- 0.67
3	120.88	127.18	6.30
4	146.65	154.08	7.43
CH_3(2,6)	24.26	23.22	- 1.04
CH_3(4)	20.35	20.16	- 0.29

Note: notations same as in Table.1.

See text for estimate of uncertainties.

Table 3.A

C-13 Chemical Shifts of the $AlBr_3$ Adducts formed with Some Alkylpyridines

Amine and C-Atoms	Free Amine Shift wrt TMS (ppm)	$AlBr_3$ Adduct Shift wrt TMS (ppm)	Coordination Shift (ppm)
Pyridine			
2	150.17	146.55	-3.62
3	123.54	126.30	2.76
4	135.34	144.62	9.28
4-ethylpyridine			
2	150.14	145.58	-4.56
3	123.22	125.67	2.45
4	152.18	163.21	11.03
CH_2	28.10	28.84	0.74
CH_3	14.27	13.28	-0.99
2,6-dimethylpyridine			
2	157.82	159.97	2.15
3	119.83	126.30	6.43
4	136.07	142.98	6.91
CH_3	24.41	27.66	3.25

Table 4

The Effects of Methyl Substitution on Ring C-13 Magnetic Shieldings in Pyridines-BF_3 Adducts

Methyl Position	Ring Carbon Position 2	3	4	Methyl Derivatives
	Ortho Effect			
2	-----	+ 2.5	-----	2-methylpyridine
2	-----	+ 3.3	-----	2,6-dimethylpyridine
3	+ 0.4	-----	- 2.7	3-methylpyridine
3	- 2.6	-----	+ 0.8	3,5-dimethylpyridine
4	-----	+ 0.6	-----	4-methylpyridine
4	-----	+ 1.0	-----	2,4,6-trimethylpyridine
	Meta Effect			
2	+ 0.5	-----	- 0.2	2-methylpyridine
2	(+ 1.5)	-----	- 1.5	2,6-dimethylpyridine
3	-----	- 0.5	-----	3-methylpyridine
3	-----	(- 0.9)	-----	3,5-dimethylpyridine
4	- 0.8	-----	-----	4-methylpyridine
4	(- 1.0)	-----	-----	2,4,6-trimethylpyridine

Methyl Position	Ring Carbon Positions 2	3	4	Methyl Derivatives
	Para Effect			
2	-----	- 3.1	-----	2-methylpyridine
2	-----	- 2.3	-----	2,6-dimethylpyridine
3	0.0	-----	-----	3-methylpyridine
3	- 3.0	-----	-----	3,5-dimethylpyridine
	Direct Substitution Effect			
2	+13.4	-----	-----	2-methylpyridine
2	+14.4	-----	-----	2,6-dimethylpyridine
3	-----	+11.0	-----	3-methylpyridine
3	-----	+10.6	-----	3,5-dimethylpyridine
4	-----	-----	+13.6	4-methylpyridine
4	-----	-----	+13.0	2,4,6-trimethylpyridine

Note: notations same as in Table.2.

( ) indicates substitution at the carbon atom.

V.3 Investigation of Surface Acidic Sites on Silica-Alumina

V.3.A. Choice of Probe Gas

The importance of a probe gas in the investigation of surface acidic sites has been pointed out earlier. The basic criteria in the choice of a probe gas are, in our NMR study, first, large chemical shifts upon adsorption on surface with respect to the neat liquid or gas. Secondly, the NMR spectra of the adsorbed probe gas have to give good resolution and signal to noise (S/N) ratio with the minimum accumulation of data (since spectrometer time and associated machinery are costly). Thirdly, and probably the most important, is that the probe gas should be able to differentiate a Lewis acid site from a Bronsted type acid site. Not many probe gases used in the past satisfy all the requirements. 2,6-di-t-butylpyridine has been used to differentiate the Lewis acidic sites as was done by Dewing et al.(55). Their infrared observations show that 2,6-di-t-butylpyridine can displace coordinately bound (to Lewis site) pyridine from an alumina

surface. They also suggest that the amine was bonded to electron-deficient oxygen species rather than the usually accepted model of coordination direct to an exposed Al^{3+}. However, Dewing's paper is a controversial one. Other workers claim that 2,6-dimethylpyridine or 2,4,6-trimethylpyridine does not bond to Lewis sites for steric reasons (56,57).

Pyridine has been used widely in literature for the investigation of surface acidic sites especially in infrared studies, as was documented by two text books (58,59) and numerous papers. From our previous study (17) and this one, pyridine is concluded not to be an ideal probe gas in C-13 NMR studies. Typical C-13 NMR spectra of pyridine adsorbed on silica-alumina are shown in Figure 5, at 0.52 and 0.76 monolayer resp. As is evident, the C4 resonance is lost in the background noise (or hidden under the huge C2 resonance) and both the C2 and C3 resonances do not have good resolution.

Caption

Figure 5.A. Carbon-13 spectrum of pyridine adsorbed on silica-alumina at 0.52 monolayer, run at 90 deg C. 15,000 scans.

Figure 5.B. Carbon-13 spectrum of pyridine at 0.76 monolayer, run at 90 deg C. 15,000 scans.

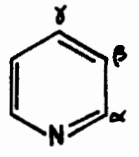

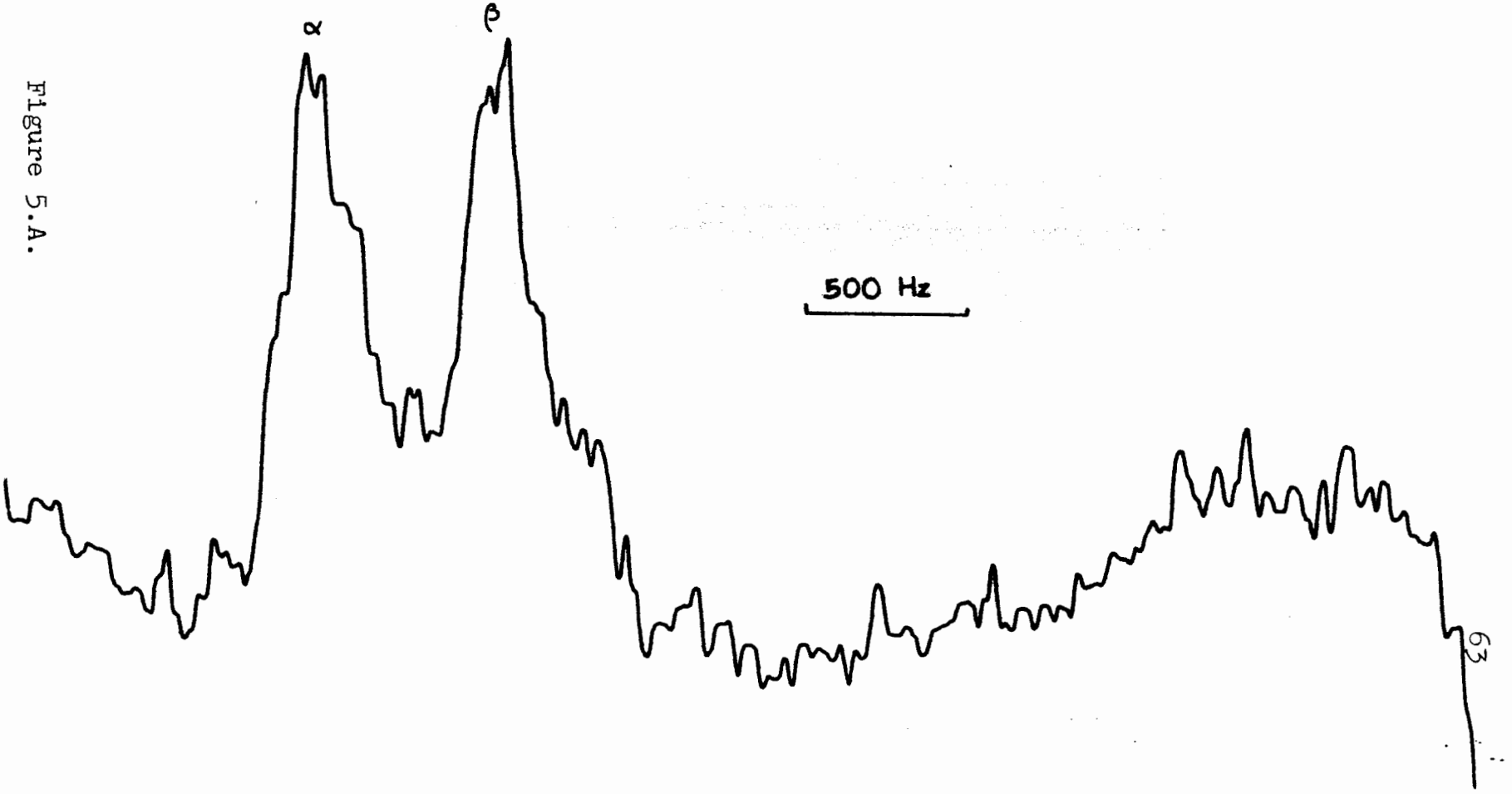

Figure 5.A.

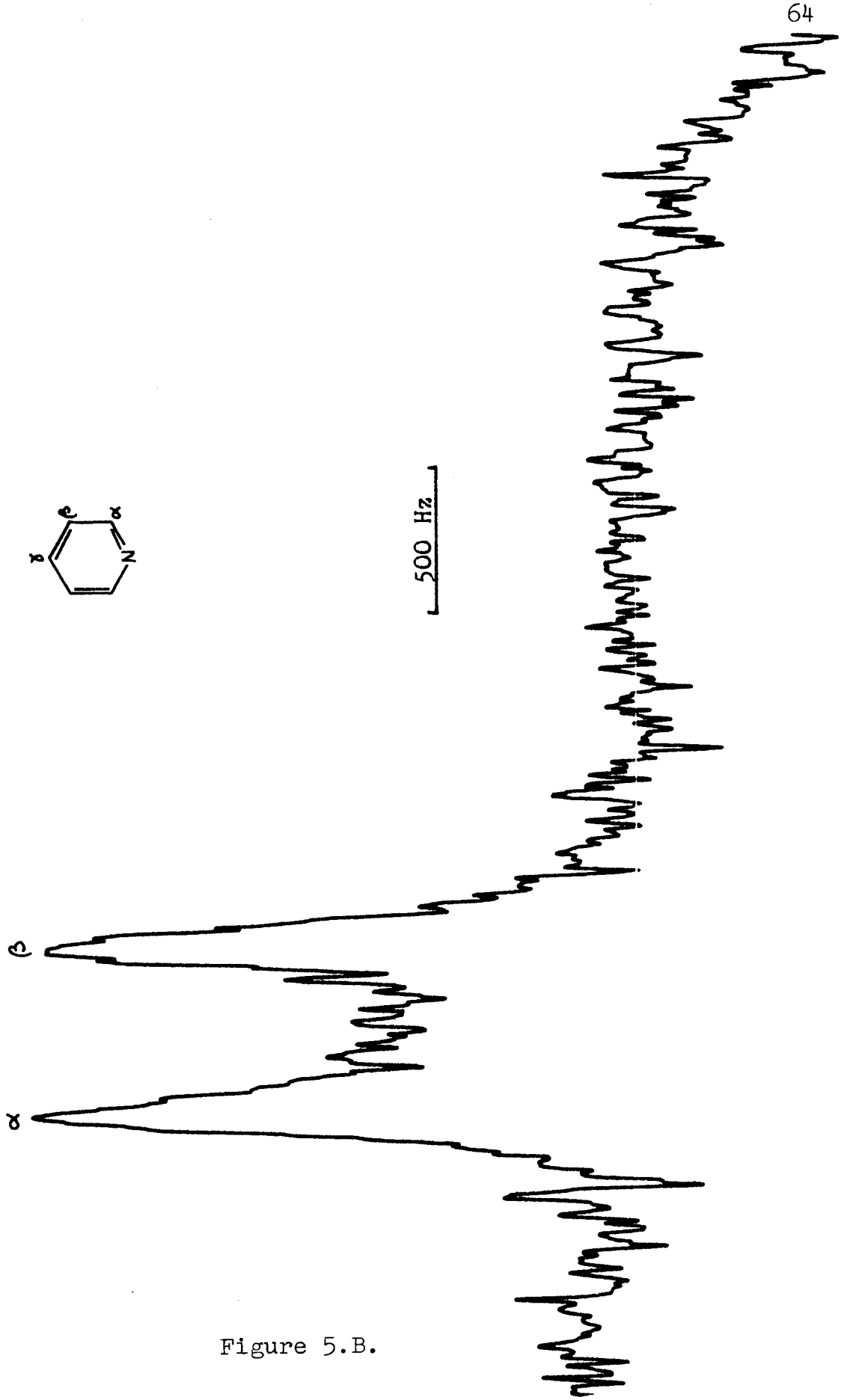

Figure 5.B.

As indicated in our previous study (17), the total number of acidic sites is related to the observed chemical shifts and total coverage (or total number of adsorbed molecules). Total coverage is always known, but difficulty in assigning the resonances would lead to uncertainty in the observed chemical shifts with a subsequent error in the calculation of total acidic sites. Therefore, pyridine is not suitable for our study.

For similar reasons, the assymetric mono-methyl-pyridines were not used. Since all five ring carbons are not equivalent, it will be difficult to resolve all resonances (since the ring carbons shift to different directions upon protonation or coordination as shown in Tables.1 and 3). Possibly , the C2 and C6 resonances will be relatively broad due to N-14 quadrupole coupling and be distinguished, but their broadness will also 'hide' the C4 resonance. C3 and C5 resonances could be assigned relatively easily due to their positions in the spectrum. But when the amine is adsorbed on the surface, these resonances will lead to a complicated spectrum due to the different chemical changes. So they are not good choices either.

The spectra of 2,6-dimethylpyridine and 3,5-dimethylpyridine are shown in Figures 6 and 7. For 3,5-dimethylpyridine, the C2 and C4 resonances are so close together that they can't be resolved. From the spectra of 2,6-dimethylpyridine, it seems to be a good choice since all resonances are relatively narrow except the C4 resonance which has a low S/N ratio, and is relatively broad. Table 5 lists the observed chemical shifts of all the carbons of 2,6-dimethylpyridine upon adsorption on silica-alumina at various coverages. But due to the small C2 and C4 chemical shift changes, 2,6-dimethylpyridine was not studied in detail.

Caption

Figure 6.A. Carbon-13 spectrum of 2,6-dimethylpyridine at 0.80 monolayer on a water-treated silica-alumina.
100,000 scans at 80 deg C.

Figure 6.B. Carbon-13 spectrum of 2,6-dimethylpyridine at 0.82 monolayer on a non-treated silica-alumina.
100,000 scans at 80 deg C.

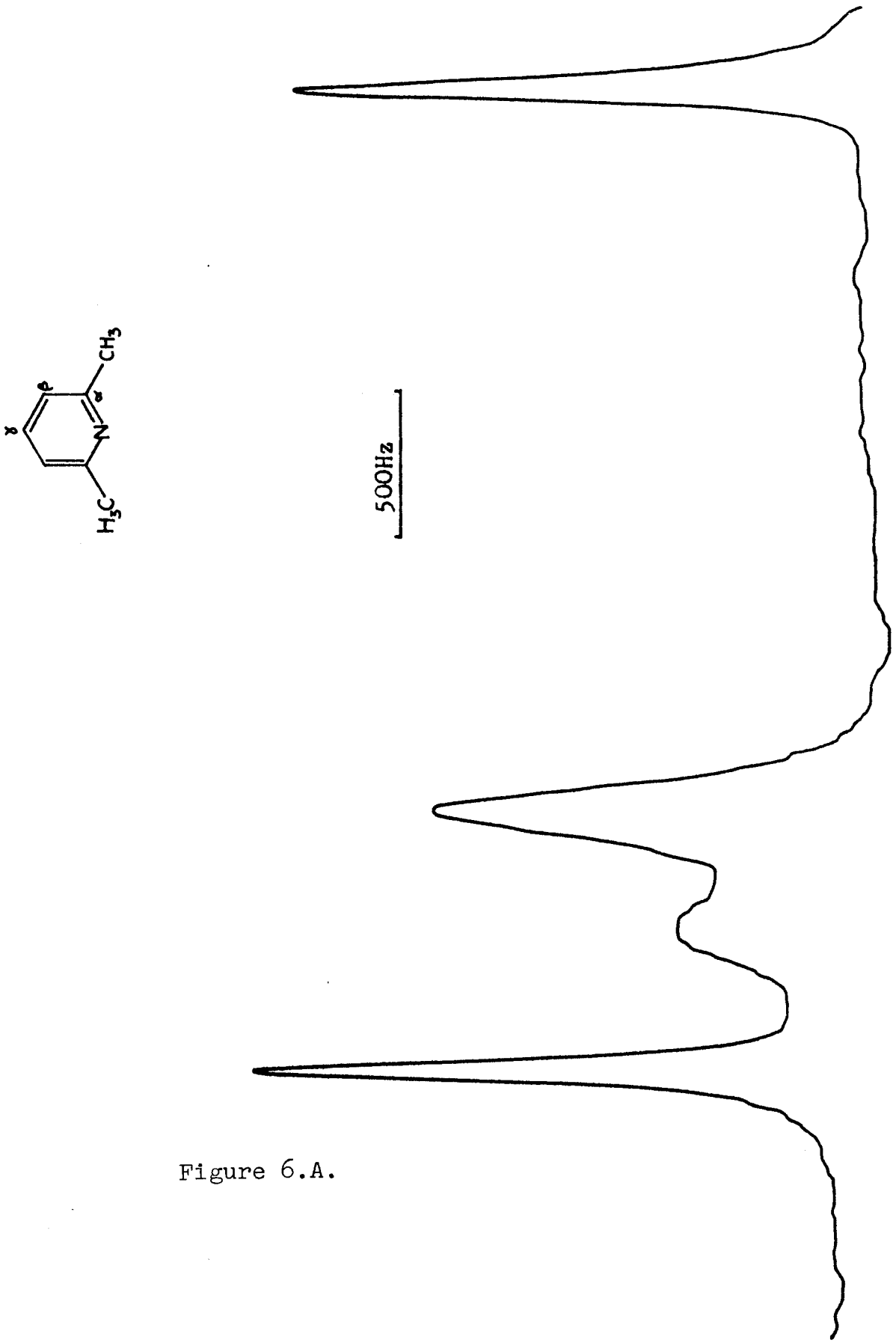

Figure 6.A.

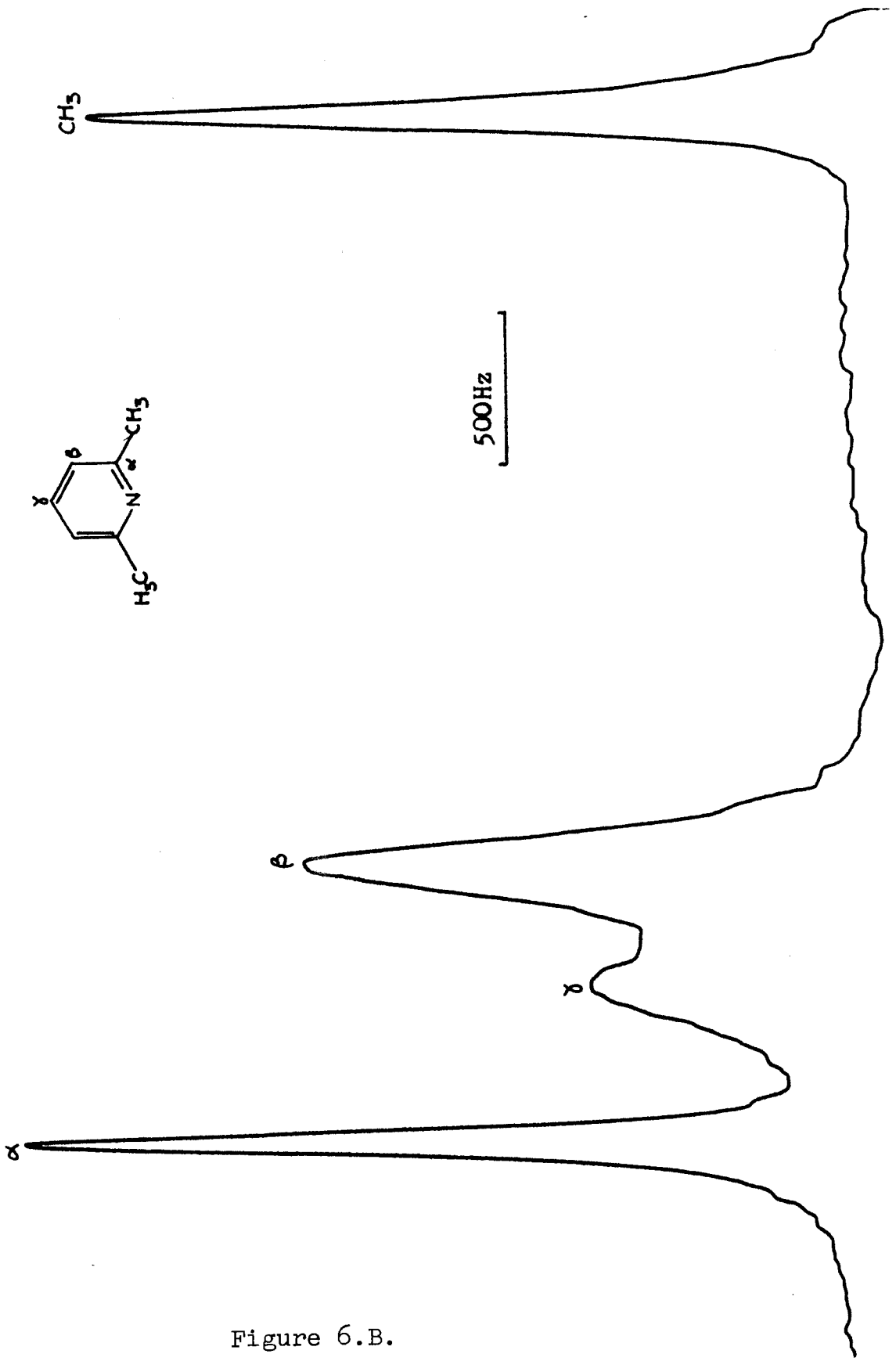

Figure 6.B.

Caption

Figure 7.A. Carbon-13 spectrum of 3,5-dimethylpyridine at 0.70 monolayer on a water-treated silica-alumina.
300,000 scans at 80 deg C.

Figure 7.B. Carbon-13 spectrum of 3,5-dimethylpyridine at 0.70 monolayer on non-treated silica-alumina.
250,000 scans at 80 deg C.

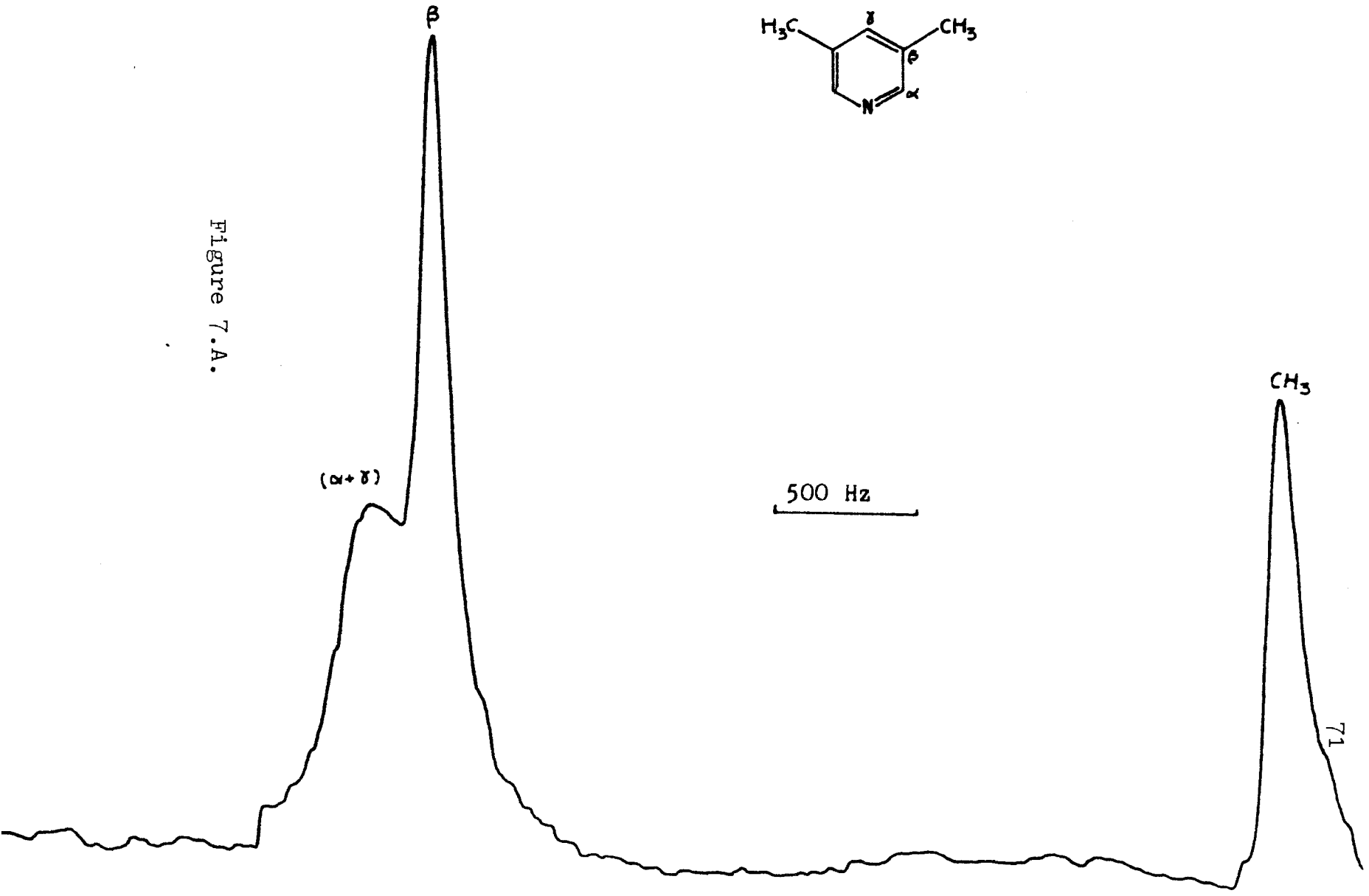

Figure 7.A.

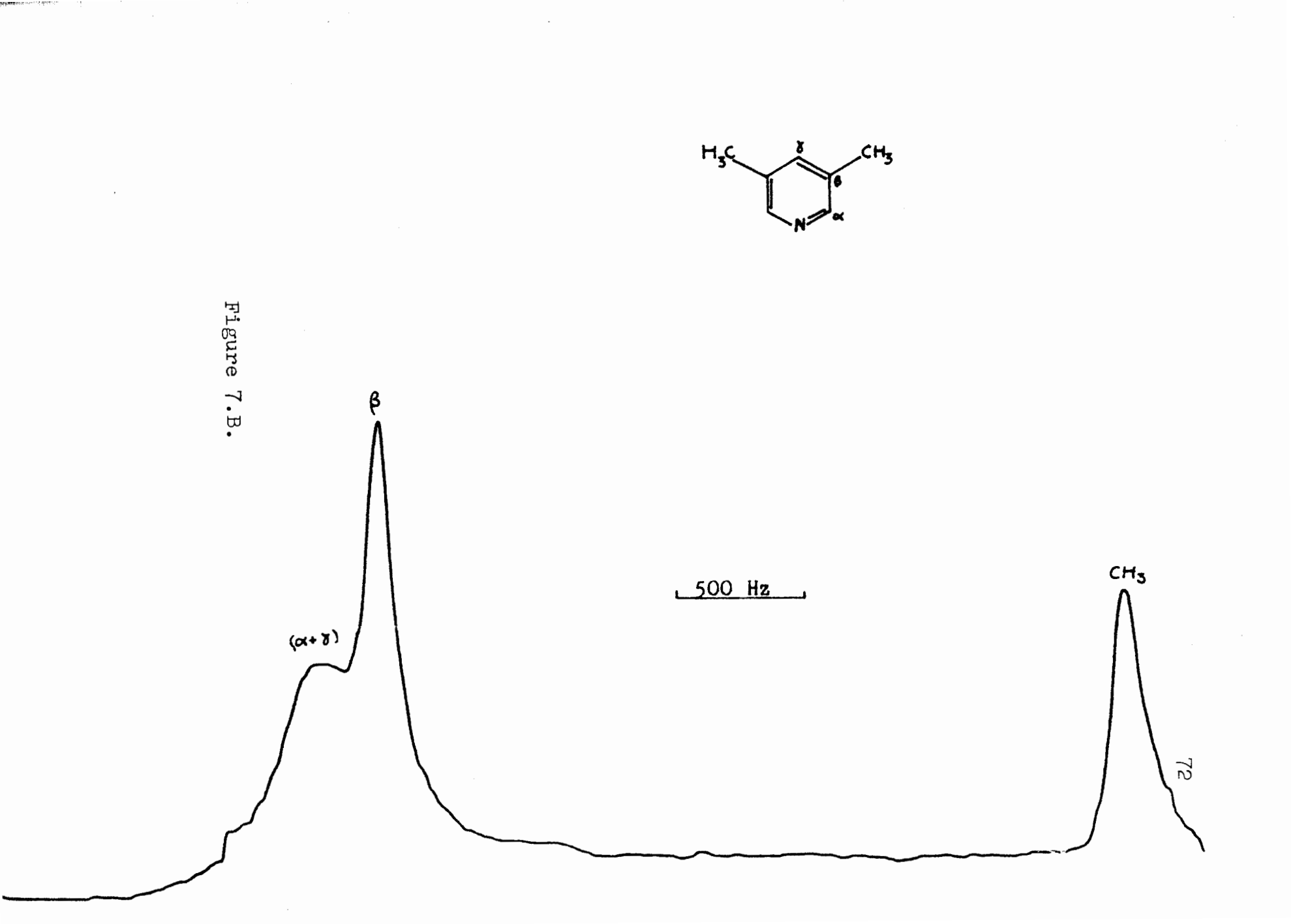

Figure 7.B.

Table 5

Chemical Shift of 2,6-dimethylpyridine on Silica-Alumina

Monolayer θ	Coverage μmole/sq.m.	Chemical Shifts C2,6	C3,5	C4	CH_3
	Non-Water-Treated				
0.58	2.38	0.1	1.3	1.0	-1.9
0.70	2.89	0.2	2.0	2.2	-1.7
0.82	3.36	0.0	1.4	2.1	-1.5
0.90	3.68	0.0	1.7	-0.1	-1.4
	Water-Treated				
0.58	2.38	-0.6	1.9	2.7	-1.9
0.69	2.82	-0.4	1.9	2.7	-2.0
0.80	3.30	-0.3	2.5	2.8	-1.6

Note: All spectra were taken at 80 deg C
Chemical shifts were obtained by subtracting the observed shift from that of neat liquid.
The water-treated sample was prepared by introduction of 3.6 μmoles H_2O/sq.m.
Minus sign in front of chemical shifts shows upfield shift. Average deviation is $\pm$ 0.3 ppm.

From Tables 1 and 3, the C2 and C4 on 4-ethylpyridine have large chemical shifts upon protonation and when coordinated to BF_3 and $AlBr_3$, so it seems to be a good candidate as a probe gas. Also, the C2 protonation and coordination shifts are relatively close, -9.1 and -7.8 ppm respectively, we may be able to obtain information out of this result. Typical spectra of 4-ethylpyridine adsorbed on differently prepared silica-alumina are shown in Figures 8 and 9.

In general, the three sets of ring carbons and the methyl resonances are well resolved. The CH_2 resonance is broad and has a low S/N ratio. Detailed study on 4-ethylpyridine adsorbed on silica-alumina is given in the next section.

Caption

Figure 8 Carbon-13 spectrum of 4-ethyl-pyridine at 0.55 monolayer on water-treated silica-alumina.
75,000 scans at 80 deg C

Figure 9 Carbon-13 spectrum of 4-ethyl-pydidine at 0.53 monolayer on non-treated silica-alumina. 15,000 scans at 80 deg C. (same figure as 3.B.)

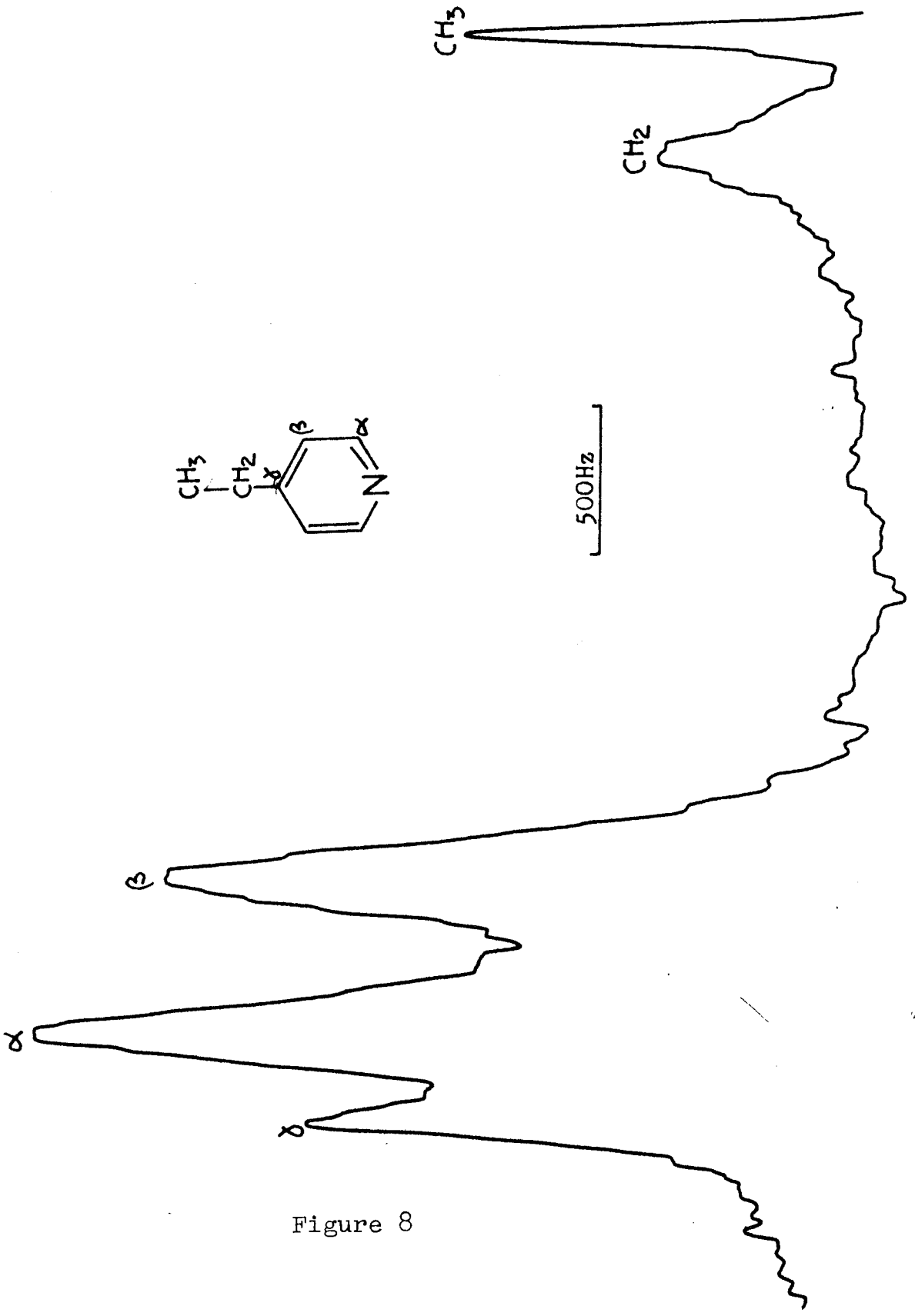

Figure 8

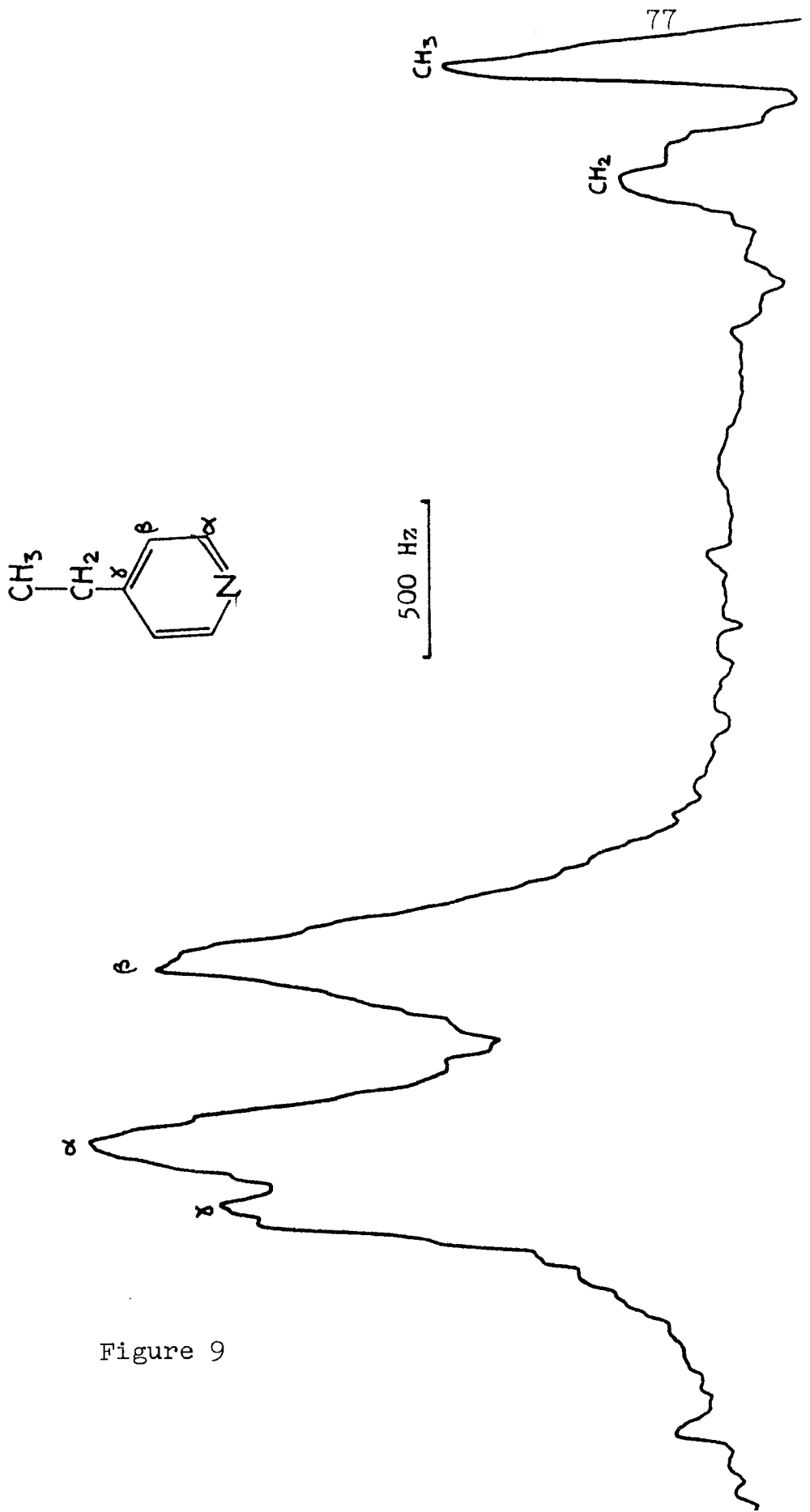

Figure 9

V.3.B Elucidation of Concentration of Surface Acidic Sites on Silica-Alumina

Tables 6 and 7 lists the observed chemical shifts of all carbons on 4-ethylpyridine when adsorbed on water-treated and non-treated silica-alumina surface respectively. For assignment of uncertainty and check for reproducibility of data, NMR spectra were repeated for one of the samples from each category. In general, the average deviation for C2 is $\pm$0.2 ppm and $\pm$0.3 ppm for C4. This large deviation is due, partly, to the time taken for each NMR run, during which the magnetic field may have drifted. The NMR spectrum of the reference amine was run before and after each experiment to measure the average drift of chemical shifts, which amounts up to $\pm$0.4 ppm depending on the length of run.

The non-water-treated silica-alumina samples were degassed at about 270 deg C and 420 deg C separately as illustrated in Table 7. There is no apparent difference between them, because the uncertainty in assigning the chemical shifts to each resonance peak ranges from 0.2 ppm

to 0.3 ppm. It is interesting to note that in Table 7, the chemical shifts of both C2 and C4 remain practically the same from 0.45 to 0.69 monolayer. This is the main reason why the plot of observed chemical shift versus inverse of coverage (see below) is so scattered. This observation is similar to that for 2,6-dimethylpyridine (from Table.5). One can actually see some sort of a maximum for the C4 chemical shift when the coverage of 2,6-dimethylpyridine on silica-alumina is from 0.7 to 0.8 monolayer.

Table 6

Observed Chemical Shifts of 4-ethylpyridine adsorbed on Water-Treated Silica-Alumina

Monolayer θ	Coverage μmole/sq.m.	Chemical Shifts C2,6	C3,5	C4	CH_2	CH_3
0.17	0.71	-7.6	3.1	8.9	-0.6	-1.4
0.27	1.11	-4.4	1.9	6.5	-1.2	-1.8
0.45	1.88	-4.3	2.1	5.5	-0.0	-1.4
0.55	2.70	-4.4	1.9	5.4	-0.3	-0.8
0.55 (*)	2.70	-4.1	1.3	6.2	-0.4	-1.9
0.69	2.88	-3.9	1.4	5.3	-0.5	-1.6
0.91	3.81	-1.9	1.6	3.9	-0.8	-1.3

Note: All notations same as Table.5

Degassing temperature at 240 to 265 deg C

(*) indicates a rerun of the same sample.

Average deviation in chemical shift $\pm$ 0.3 ppm

Table 7

Observed Chemical Shifts of 4-ethylpyridine adsorbed on Non-water Treated SiO_2-Al_2O_3

Monolayer θ	Coverage μmole/sq.m.	Chemical Shift (ppm) C2,6	C3,5	C4	CH_2	CH_3
	Degassed at 260-285 deg C					
0.40	1.71	-3.2	2.5	3.8	1.3	-1.0
0.53	2.22	-2.2	2.6	3.5	0.4	-1.7
0.77	3.22	-1.1	1.9	3.1	0.0	-0.8
0.91	3.78	-2.0	0.7	2.9	-1.8	-1.4
0.91 (*)	3.78	-1.9	0.6	3.3	-1.3	-1.4
	Degassed at 422 deg C					
0.58	2.41	-2.9	2.0	4.1	-0.3	-1.8
0.76	3.17	-2.1	1.2	3.0	-1.2	-1.3
0.91	3.78	-1.5	1.5	2.5	-0.4	-0.6

Note : All notations same as previously described.

Average deviation in chemical shift $\pm$ 0.3 ppm

The water introduced into the water-treated silica-alumina ranged from 3.12 to 3.85 μmole/sq.m. The amount of water adsorbed will be sufficient to rehydrate the oxide surface with the formation of SiOH type structure as pointed out by Schreiber and Vaughan (32). There will also be an inversion of acid-site densities. Parry (22) and Basila et al.(28) found that the Lewis site concentration decreases and the Bronsted site concentration increases upon rehydration. This inversion is believed to be due to the conversion of Lewis sites to Bronsted sites.

V.3.C. Interpretation: Linear Model 1.

From previous results in this laboratory (17,53), we concluded that observed chemical shifts reflect the concentration of surface sites. From solution data (Tables 1 and 3), we observed that the protonation and coordination shifts of the C2 on 4-ethylpyridine are close together (-9.1 and -7.8 ppm respectively). Thus we can assume an average acidic shift for both. If this is done, then the C2 shift of 4-ethylpyridine could be shown to reflect the concentration of total acidic sites on silica-alumina because it will give the same average shift when adsorbed on a Bronsted or a Lewis site.

If we furthur assume that the observed chemical shifts relate to coverage as in (17), we can write

$$[V.1] \quad \delta_{obs}^{C2} = \frac{n_+}{n_T}\delta_+^{C2} + \frac{n_L}{n_T}\delta_L^{C2} + \frac{n_N}{n_T}\delta_N^{C2}$$

where δ_{obs}^{C2} is the observed C2 chemical shift, δ_+^{C2}, the protonation shift for C2, δ_L^{C2}, the coordination shift of C2, n_T the total moles of molecules adsorbed onto the surface, n_+, the number of moles of amines bonded

to Bronsted sites, n_L, the number of moles of amines bonded to Lewis sites and n_N, the number of moles of amines physically adsorbed on the surface (or to non-acidic sites). And finally δ_N^{C2}, the chemical shift that would be obtained for C2 for physically adsorbed 4-ethylpyridine molecules (which is equal to -0.9 ppm --- the data from SiO_2 experiment).

Notice that this model assumes:

1) The number of Bronsted and Lewis acidic sites are fixed on the surface of silica-alumina.
2) The probe gas (4-ethylpyridine) either interacts with an acidic site or doesn't (i.e. to a non-acidic site).
3) The observed chemical shift is a weighted average of the populations of 4-ethylpyridine interacting with Bronsted, Lewis or non-acidic sites.
4) Chemical shifts of these three kinds of 4-ethylpyridine molecules are given by values with BF_3 adducts (δ_L), aqueous HCl (δ_+) and with SiO_2 (δ_N) respectively.

Using these assumptions and assuming that the δ_+ and δ_L can be averaged to give a total acidic shift of -8.5 ppm, [V.1] becomes

[V.1.A] $$\delta_{obs}^{C2} = -8.5\left(\frac{n_A + n_L}{n_T}\right) - 0.9\frac{n_N}{n_T}$$

Since the sum of $(n_+ + n_L)$ should give the total number of moles of 4-ethylpyridine bonded to acidic sites (n_A) and from Assumption.2 n_T would be given by the sum of $n_A + n_N$, after simple algebra, we would get

[V.2] $$\delta_{obs}^{C2} = -\frac{n_A}{n_T}(7.6) + 0.9$$

Substituting data from Tables 6 and 7, we will obtain Tables 8 and 9.

Table 8

Fraction and Number of Moles of Acidic Sites for Non-treated Surface.

Coverage μmole/sq.m	δ^{C2}_{obs} ($\pm$0.2)	$f_A=n_A/n_T$ ($\pm$ 0.04)	n_A(μmole/sq.m) ($\pm$ 0.2)
1.71	-3.2	0.30	0.5
2.22	-2.2	0.17	0.4
3.22	-1.1	0.03	0.1
3.78	-2.0	0.14	0.6
3.78	-1.9	0.13	0.5
2.41	-2.9	0.26	0.6
3.17	-2.1	0.16	0.5
3.78	-1.5	0.08	0.3
Average	=	--- (*)	0.4

Note: (*) denote no average can be taken. See text.

Table 9

Fraction and Number of Moles of Acidic Sites for Water-treated Silica-alumina

Coverage μmole/sq.m	δ^{C2}_{obs} ($\pm$0.2)	$f_A=n_A/n_T$ ($\pm$ 0.04)	n_A(μmole/sq.m.) ($\pm$ 0.2)
0.71	-7.6	0.88	0.6
1.11	-4.4	0.46	0.5
1.88	-4.3	0.45	0.8
2.70	-4.4	0.46	1.2
2.70	-4.1	0.42	1.1
2.88	-3.9	0.39	1.1
3.81	-1.9	0.13	0.5
	Average =	---(*)	---(*)

Note: (*) denote no average can be taken, see text.

The values obtained in Table 8 are almost consistent except the anomalous values of f_A= 0.03 and n_A= 0.1μmole/sq.m. While for Table 9, abnormality is observed, which is not found in Table 8. The apparent increase in n_A values from coverage of 0.71 to 2.70 μmoles/sq.m. is of course due to the region of almost constant chemical shift changes. Viewed at face value, one might say that in this region, n_A/n_T is controlled by an equilibrium, rather than by the total number of acidic sites. This would imply a substantial amount of weak acidic sites (of the approximate strength of 4-ethylpyridine) to be present on the surface, which is at variance with previous results (12). Therefore we could conclude at this stage that n_A = (0.4$\pm$0.2) μmoles/sq.m. for non-treated silica-alumina and no value for the water-treated surface. However if the uncertainty is increased to $\pm$ 0.4, then n_A for the water-treated samples can be averaged as (0.9$\pm$0.4)μmoles/sq.m.

Our primary goal is to elucidate the concentration of each type of acidic sites separately. Apparently, we are limited by Model 1 that only the total acid sites are found. That is how Model 2 differs from the above---we actually have more than one parameter.

V.3.D. Linear Model 2

As could be seen in Tables 1 and 3, the C4 shifts of 4-ethylpyridine upon protonation and coordination are quite different (14.5 and 9.5 ppm respectively). The observed C4 chemical shift of 4-ethylpyridine when adsorbed on silica-alumina never exceeds the protonation shift nor the coordination shift even at 0.17 monolayer (a very low coverage indeed). So we could assume that the amount of adsorbed 4-ethylpyridine exceeds all available acid sites on the surface. If this is the case, then we could assume that the observed chemical shift is an average shift of the rapidly exchanging 4-ethylpyridine molecules among the acidic sites and the non-acidic sites (where we would observe physically adsorbed 4-ethylpyridine). If this assumption is valid and with the four basic assumptions listed for Model 1, we could relate the fractional number of protonated molecules (f_+), fractional number of coordinated molecules (f_L) and fractional number of physically adsorbed molecules (f_N) by :

[V.3] $$\delta_{obs}^{C4} = \delta_{+}^{C4} f_{+} + \delta_{L}^{C4} f_{L} + \delta_{N}^{C4} f_{N}$$

where δ_{obs}^{C4} is the observed C4 chemical shift and δ_{+}^{C4} is the observed protonation shift, δ_{L}^{C4}, is the observed coordination shift, and δ_{N}^{C4} is the C4 chemical shift that would be observed for physisorbed 4-ethylpyridine, which is equal to 1.5 ppm from previous argument for δ_{N}^{C2} value.

Further assuming that the previous calculations may not be correct, i.e. by assuming that the observed C2 chemical shift reflects the total acidity, we can then write a similar equation as [V.3] relating C2 chemical shifts as

[V.4] $\delta_{obs}^{C2} = \delta_{+}^{C2} f_{+} + \delta_{L}^{C2} f_{L} + \delta_{N}^{C2} f_{N}$

with the same notations. Substituting δ_{+} and δ_{L} values for C2 and C4 from Tables 1 and 3 and δ_{N} values from the data of adsorbed 4-ethylpyridine on silica, we can then re-write [V.3] and [V.4] as

[V.3.A] $\delta_{obs}^{C4} = 14.5\ f_{+} + 9.46\ f_{L} + 1.5\ f_{N}$

[V.4.A] $\delta_{obs}^{C2} = -9.1\ f_{+} - 7.89\ f_{L} - 0.9\ f_{N}$

Adding and subtracting [V.3.A] and [V.4.A], we get

[V.5.A] $\delta_{obs}^{C4} + \delta_{obs}^{C2} = 1.57\ f_{L} + 5.4\ f_{+} + 0.6\ f_{N}$

[V.5.B] $\delta_{obs}^{C4} - \delta_{obs}^{C2} = 17.35\ f_{L} + 23.6\ f_{+} + 2.4\ f_{N}$

We know that f_+, the fraction of protonated molecules, is equal to

[V.6.A] $f_+ = n_+/n_T$

and similarly

[V.6.B] $f_L = n_L/n_T$ and

[V.6.C] $f_N = n_N/n_T$

where n_+, n_L and n_N are the number of moles of protonated molecules, coordinated molecules and physisorbed molecules respectively, and n_T is the total moles of chemisorbed 4-ethylpyridine.

Also, we know that

[V.7] $n_A = n_+ + n_L$

where n_A is the total mole of acidic sites, and

[V.8] $n_T = n_A + n_N$

based on the assumption that the adsorption sites are of two kinds only: acidic and non-acidic, and that the acidic sites are of two kinds: Bronsted and Lewis types only.

Substituting [V.6], [V.7], and [V.8] into [V.5.A] and [V.5.B], we arrive at

$$[V.9.A]\ \delta^{C4}_{obs} + \delta^{C2}_{obs} = 1/n_T[\ 0.97xn_A + 3.83xn_+] + 0.6$$

$$[V.9.B]\ \delta^{C4}_{obs} - \delta^{C2}_{obs} = 1/n_T[14.95xn_A + 6.25xn_+] + 2.4$$

With each datum from Tables 6 and 7 for the non-treated and water-treated surface, we have a pair of simultaneous equations, that we could solve. The results are shown in Tables 10 and 11.

Table 10

n_A and n_+ values for non-treated silica-alumina surface

δ^{C2}_{obs}	δ^{C4}_{obs}	n_T	n_A	n_+
		(μmoles/sq.m.)		
-3.2	3.8	1.71	(*)	---
-2.2	3.5	2.22	0.4	0.3
-1.1	3.1	3.22	(*)	---
-2.0	2.9	3.78	0.6	0.2
-1.9	3.3	3.78	(*)	---
-2.9	4.1	2.41	0.7	0.2
-1.9	3.3	3.17	0.5	0.1
-1.5	2.5	3.78	(*)	---
		Average =	0.6	0.2

Note: Deviations for n_A and $n_+ = \pm 0.2\mu$moles/sq.m.
(*) denotes rejected values i.e. $n_+ > n_A$ or values of n_A which lead to negative values of n_+ .

Table 11

n_A and n_+ values for water-treated silica-alumina surface

δ^{C2}_{obs}	δ^{C4}_{obs}	n_T	n_A	n_+
			(μmoles/sq.m.)	
-7.6	8.9	0.71	(*)	---
-4.4	6.5	1.11	0.5	0.3
-4.3	5.5	1.88	0.9	0.1
-4.4	5.4	2.70	(*)	---
-4.1	6.2	2.70	1.1	0.8
-3.9	5.3	2.88	1.2	0.3
-1.9	3.9	3.81	(*)	---
		Average =	0.9	0.4

Note: Deviations for n_A and n_+ = $\pm$ 0.2 moles/sq.m.

Other notations same as in Table 10.

The above calculation is more realistic in the sense that it only assumes that the observed chemical shifts (of C2 and C4) are average shifts of the rapidly exchanging 4-ethylpyridine molecules among all the acidic and non-acidic sites, which is valid from previous publications of this laboratory (17,54).

However, as could be observed from Tables.10 and 11, only 50% of the results are physically meaningful (the others are all rejected due to non-physical characteristics: n_+ values less than n_A values etc.) This anomalous trend is again, a reflection of the fluctuating chemical shifts observed with respect to coverages.

We could summarize our results with comparison to literature values as follows in Table.12.

We notice that our values for the non-treated samples fall quite close to the literature values for both total acidic sites and Bronsted sites concentration, but not for the water-treated samples. This may arise from some defects in our models.

Table 12

Elucidated total acidic sites (N_A)

and number of protonated sites (N_+)

Groups	Total Acidic Sites x 10^{13} per sq.cm.	Bronsted Sites x10^{13} per sq.cm.
Schwarz (61)	3.4	1.1
	3.3(rehyd)	2.3(rehyd)
Basila & Kantner (28,30)	12.4	1.8
Scokart et al. (62)	4.1	---
Clark & Holm (60)	3.5	---
Ours		
Model 1	2.4	---
	5.4(rehyd)	---
Model 2	3.6	1.2
	5.4(rehyd)	2.4(rehyd)

Note: rehyd= rehydrated samples.

V.3.E. Defects in the Models.

The flaw in these two linear models and the four basic assumptions are demonstrated by the following observations: first, some data in Tables.6 and 7 lead to negative amounts of Lewis acid in Tables.10 and 11. Secondly, in case of water-treated samples, total acid appears to increase with coverage. This is caused by the nearly constant chemical shift changes for coverage from 1.1 to 2.9μmole/sq.m. And thirdly, total concentration of acidic sites seems to increase with added water. One would have expected that there is a conversion of Lewis sites to Bronsted sites with total acid concentration constant (22,28,30,61).

Apparently, both of these two linear models are not applicable in the present observation on silica-alumina. Plots of observed C2 and C4 chemical shifts from Tables 6 and 7 versus the inverse of coverages are shown in Figures 10 and 11. In general, the plot of C4 vs 1/coverage is quite linear after least square fit, except for the non-treated samples. The two degas-

Figure 10 Plots of Observed C2 Chemical Shifts versus 1/Coverage for Non- and Water-Treated Silica-Alumina Surface.

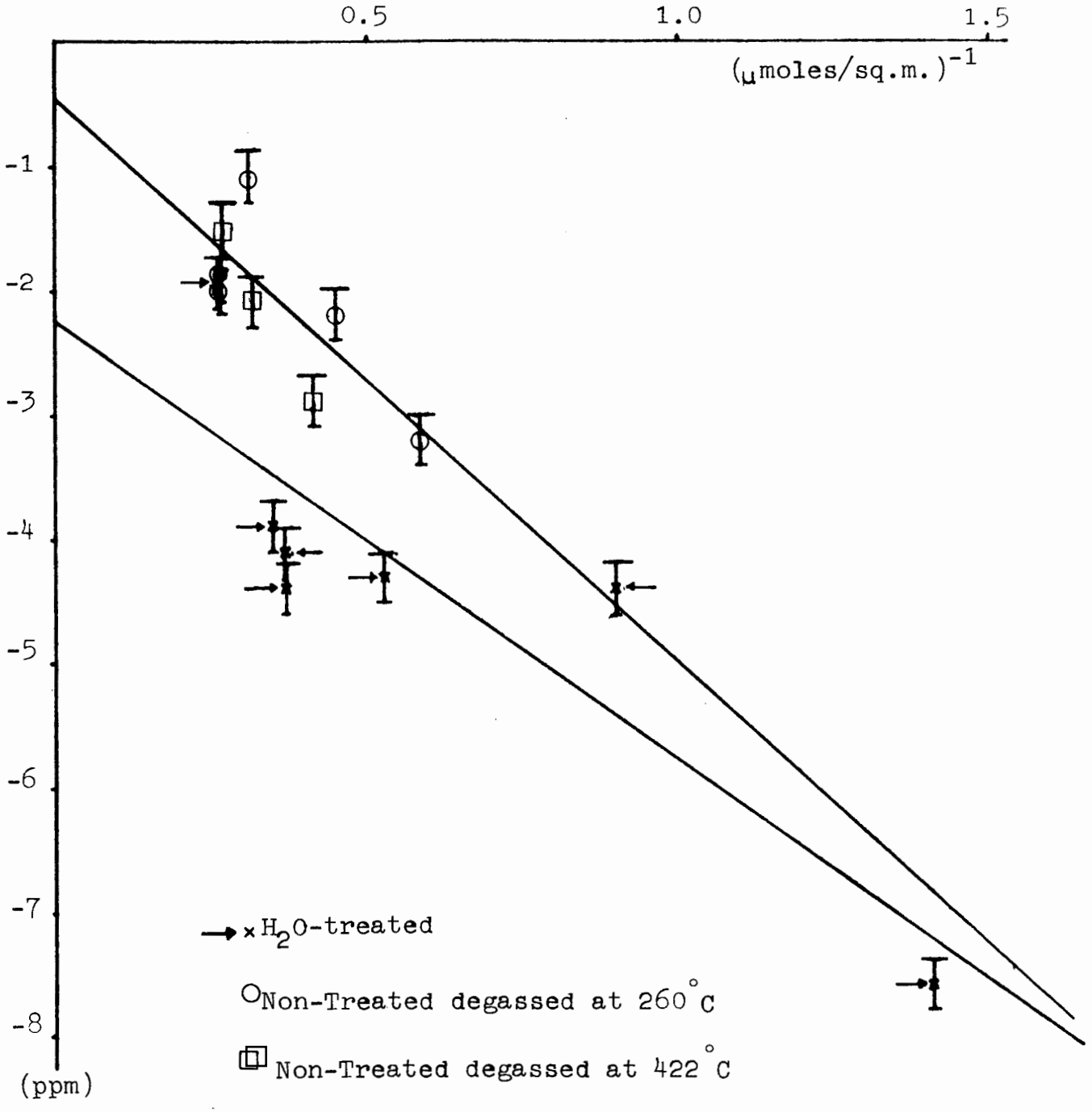

Figure 11 Plots of Observed C^4 Chemical Shifts versus 1/Coverage for Non- and Water-Treated Silica-Alumina Surface.

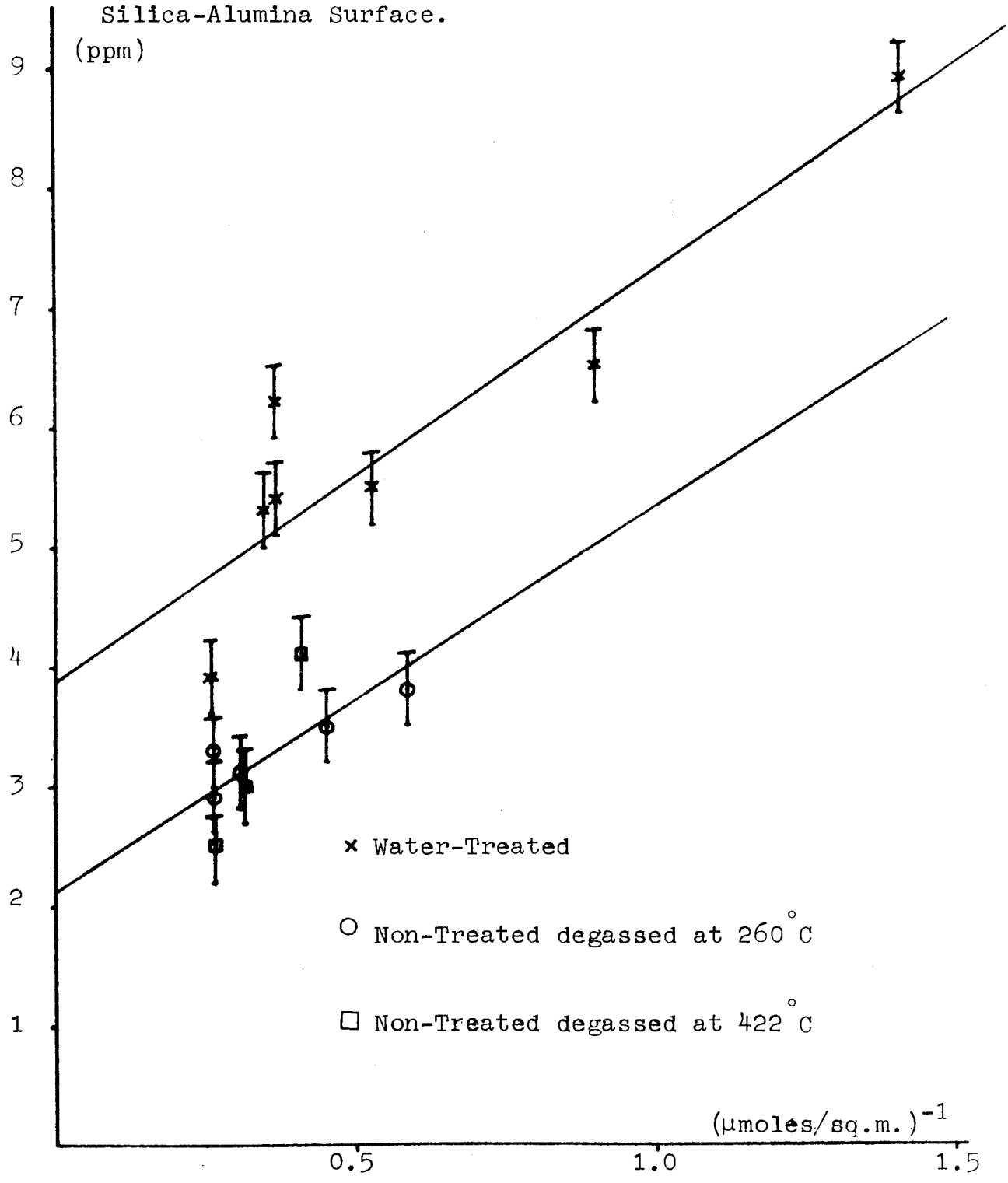

sing temperature (at 260 and 422°C) seem to have some effects on the observed chemical shifts, and the scattering of data points is not compensated by the errors associated with the observed chemical shifts. While for the C2 plot, there is a clear deviation from linearity. For the water-treated samples, the points on the graph clearly demonstrate a sigmoidal characteristic, and it may be too optimistic to try to fit a straight line through them. The data points for the non-treated samples also show a poor fit for a straight line. More data points on the observed C2 and C4 chemical shifts are required for a clear demonstration of the shape of the curve for both plots. However due to instrumental and time limitations, this is not possible, the reasons being given earlier under Apparatus in Chapter IV.

Based on the above discussion, the system of adsorbed 4-ethylpyridine on silica-alumina seems more complex than predicted by earlier studies (17) from this laboratory and other similar studies in the literature using other physical techniques (titration or IR study). Apparently a more complex mathematical model is required to express the dependence of observed chemical shifts on coverages, if such relationship exists.

The few possibilities why this linear correlation breaks down may be due to the following :

(1) There is an equilibrium reaction of the acidic sites on the surface with the amine. Although silica-alumina is believed to have strong acidity, yet recent titration experiments by Damon et al.(64) registered a distribution of acidic sites with varying acid strength. Refering to Damon's data, the acid strength for our sample could range from 4.75 to -6.63. The possible implications are:

i) Since we didn't observe separate resonance lines for each carbon, therefore the observed chemical shift is an average of all populations of 4-ethylpyridine interacting with sites of different acid strength with different equilibrium constants, which is believed to yield the fluctuating chemical shifts changes that were observed.

ii) The different chemical shift changes observed for the same sample when measured again could be a direct result of this equilibrium, ignoring different experimental and instrumental conditions.

Although the above discussion may seem reasonable, no quantitative justification could be obtained due to the unknown nature of the surface of this catalyst. But one thing for sure is that if such equilibrium exists, it may be wholly responsible for the fluctuations in the observed chemical shifts.

(2) Another possible defect would be the assignment of coordination shift. As could be seen in Tables.3 and 3A the coordination shift of the BF_3 and $AlBr_3$ adducts with 4-ethylpyridine are significantly different. Again these data are different from other sources such as those of Lavallee et al.(19) who measured the chemical shifts of pyridines coordinated to Rh(III) and Co(III), and Cushley et al.(65) who measured chemical shifts of aromatic N-oxides.

These differences in coordination shifts may reveal the difference in steric hindrance and acid strength of the Lewis acid sites on silica-alumina. We may speculate that at low coverage, the adsorbed amine would be coordinated preferentially to sites with less steric

hindrance (BF_3 type) and then to greater steric hindrance sites ($AlBr_3$ type) as coverage increases. This may be represented by a transition in the observed chemical shifts on the plots shown in Figures. 10 and 11 with a sigmoidal shape curve.

If this speculation is valid, the model expressing the relationship between chemical shifts and coverages will be more complex because now it contains more terms (i.e. the fractional population of amines bonded to different Lewis sites with varying steric hindrance and acid strength).

While the assignment of coordination shift for the adsorbed amine is questionable, the assignment of protonation and physisorption shifts seem reasonable. In view of recent studies (53,56) and older ones (22,28) that the chemical shifts of protonated adsorbates are the same as those observed in acidic solution, therefore the assignment of protonation shift is accurate. For the shift of a physically adsorbed amine on silica-alumina, it shouldn't differ too much from that sorbed

on pure silica gel by 0.2 to 0.3 ppm. So the assignment of coordination shift may be the flaw in our linear models.

(3) Solvent effects have been studied effectively by means of NMR. Recent study by Litchman (67) has pointed out that specific interactions among different molecules can also produce a solvent effect. Therefore the effect of the two possible interactions on the surface such as adsorbate-water, adsorbate-adsorbate interactions can be approximated as a dilution of adsorbed amine by water or an inert solvent such as $(CH_3)_4C$.

However, this approximation is over-simplified, because in the liquid state, the amine molecules are surrounded by solvent molecules but in the adsorbed state, it is only a two-dimensional problem. Therefore, only a qualitative discussion of these interactions can be given.

The first interaction, i.e. the adsorbate-water interaction is important only in water-treated samples because for the non-treated samples, after the degassing procedure most of the surface water would be removed (53,55). Also only solvent effect data are available for pyridine, we have to assume a similar effect for 4-ethylpyridine. Since the amounts of water and the 4-ethylpyridine adsorbed are known, the amount of dilution can be calculated and the effect on chemical shift changes can be extrapolated from Litchman's data (67). The results are shown in Table 13.

Table 13

Solvent Effect of Water on Chemical Shifts of the Adsorbate--Silica-Alumina System

Coverage 4-ethyl pyridine μmole/m^2	Coverage H_2O μmole/m^2	Mole % 4-ethyl pyridine	C2 Shift changes (ppm)	C4 Shift changes (ppm)
0.71	3.73	16	-1.27	1.62
1.11	3.70	23	-1.17	1.50
1.85	3.80	33	-1.06	1.38
2.70	3.73	42	-0.89	1.18
2.70	3.73	42	-0.89	1.18
2.88	3.64	44	-0.86	1.14
3.81	3.85	50	-0.77	1.04

Note: (-)ve sign indicates upfield shift.
(+)ve sign indicates downfield shift.
Data from Table 6.

Apparently, the solvent effect is appreciable for water-adsorbate interactions ranging from 1 to 1.6 ppm for C4 shift and -0.8 to -1.3 ppm for C2 shift. Notice that the upfield shift for C2 and the downfield shift for C4 is the same as that for adsorbed species. Therefore the solvent effect has a net effect of enhancing the observed chemical shifts for the adsorbed species, by an average of -1 ppm for C2 and 1.3 ppm for C4 shift.

Since δ_N^{C2} = -0.9 ppm and δ_N^{C4} = 1.5 ppm from 4-ethylpyridine on silica experiment, the amine-water complex would just look like more non-bonded amine i.e. amines bonded to non-acidic sites which would imply some change in the numbers (n_N), but would not cause the model to break down.

However a quantitative justification of how strong this interaction is cannot be obtained, because :

i) The water molecules may be chemisorbed on the surface also, thus reducing the amount hydrogen-bonded to the adsorbed amine molecules.

ii)Since this adsorption system is significantly different from the liquid state, the chemical shift changes given for solvent effect in Table.13 may not be justifiable.

For the adsorbate-adsorbate interaction, we can do it in a naive way--- by assuming that the adsorbates are effectively 'diluted' with an inert solvent like neopentane,$(CH_3)_4C$.

In the calculation of the concentration of the solvent,$(CH_3)_4C$, we obtain an area of 38 A^2 per molecule by deducing from liquid density and assuming a spherically shaped molecule. Further assuming that this 'solvent' occupies the rest of the area on the surface, not occupied by the adsorbed 4-ethylpyridine, the amount of $(CH_3)_4C$ on the surface can be calculated. The problem can then be approximated as a solvent (neopentane)-- solute (4-ethylpyridine) dilution system. The effect on C2 chemical shift upon dilution is almost constant at about 0.05 ppm from 0 to 100% dilution extrapolated from Litchman's data (67). However, a slight effect is observed for the C4 chemical shift, and they are tabulated in Tables.14 for non- and water-treated samples.

Table 14

Adsorbate-Adsorbate Interactions in the System of 4-ethylpyridine on Silica-Alumina

Coverage (μmole/sq.m.)		Mole %	C4 Shift
4-ethyl pyridine	H_2O	4-ethyl pyridine	Changes (ppm)
Water-treated			
0.71	3.63	16	-0.94
1.11	3.20	26	-0.80
1.88	2.41	44	-0.54
2.70	1.97	58	-0.33
2.70	1.97	58	-0.33
2.88	1.36	68	-0.19
3.81	0.39	91	0.14
Non-treated			
1.71	2.58	41	-0.59
2.22	2.06	52	-0.42
3.22	1.01	76	-0.07
3.78	0.39	91	0.14
3.78	0.39	91	0.14
2.41	1.84	57	-0.35
3.17	1.05	75	-0.08
3.78	0.39	91	0.14

Note: same notation as in Table 13.

Results from non-treated samples show a very small effect upon interactions among adsorbates, and they can be accounted for by experimental and instrumental errors except at coverage of 1.71 and 2.22 μmoles per sq.m. Larger effects are observed for the water-treated samples. Notice that the dilution in this case does not include the presence of water molecules, therefore the solvent effect in this case should be smaller than those given in Table 14. If water concentration has to be included into the calculation, we would be considering a very complicated heterogeneous system, and net solvent effect could not be obtained.

Therefore the adsorbate-adsorbate interaction is very small indeed. Other interactions such as the local effects of adsorbate-surface binding and possible surface structure defects caused by adsorbate binding are difficult to evaluate, since they involve the exact structure of the surface of silica-alumina. Water molecules adsorbed on the surface are expected to cause some change on the surface structure e.g. converting Lewis sites to Bronsted sites (28,30,61), but this effect is not well demonstrated in this study.

V.3.F Construction of a Possible Surface Model

We could estimate the Al atoms on the surface by the following naive way. Since the ratio of Al atoms to Si atoms in this silica-alumina is 32%, therefore, there are about two Al atoms in every thirteen O atoms. Assumeing that the surface O atoms are hexagonally close-packed with ionic radii of 1.40 A, there would then be 2.3×10^{14} Al atoms per sq.cm. All of these Al atoms would be residing in the tetrahedral holes among the O atoms if we assume that the Al atoms are situated in the Si position after an isomorphous substitution in the silica lattice for the Si atoms.

If this simple model is accepted, we are faced with an immediate question: if all the Al atoms are the sole contributors to the acidic sites on the surface, why wouldn't our results in Table 12 approach the number of Al atoms?

To explain this, we have to go back to Figure 1 and 2 for the surface structures of Bronsted sites and Lewis sites.

So far, only tetrahedral silica and tetrahedral alumina have been considered. In octahedral alumina i.e.

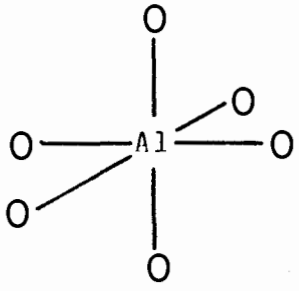

each Al-O line represents one half of a valence unit. Silica can 'react' with such a system

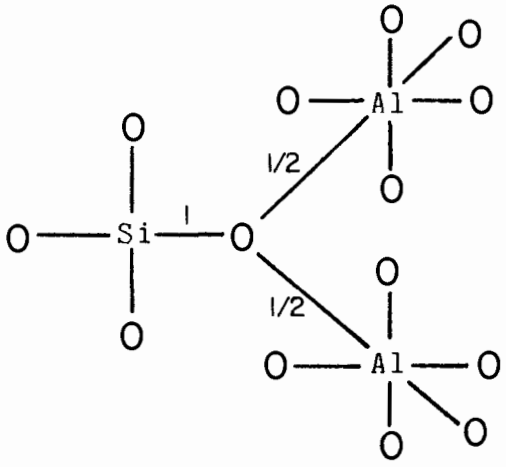

so that each oxygen shares one tetrahedral silicon atom and two octahedral aluminum atoms. This produces a saturated aluminum silicate that should have no acidity (26). Simple calculation reveals that the number of this kind of oxygen (three-coordination) exceeds the number of Al atoms on the silica-alumina surface, so that it is not surprising that most of the Al atoms exist in this form.

To summarize, on the silica-alumina surface, there is an upper limit of about 1.7×10^{14} Al atoms per sq.cm. which are non-acidic due to packing and/or tetra-coordination so that they could not be converted to acidic sites. The other Al atoms exist as Bronsted or Lewis acidic sites, depending on the treatments of the surface. However due to the lack of an appropriate model for interpretation of data, the exact concentration of each kind of acidic sites could not be ascertained.

Chapter VI

VI. Conclusion and Future Study

In this study, we are able to establish three facts. First, pulse and Fourier transform NMR spectroscopy is suitable for surface study provided the adsorbate-adsorbent interactions are not too strong so that adsorbate on different kinds of active sites could rapidly exchange themselves with the result of an average shift, and that the spectral lines are not excessively broad.

Secondly, the importance of a probe gas is illustrated. 4-ethylpyridine is by no means the best available, and hopefully in the future, we can find a more specific probe gas which could distinguish among sites, e.g. some base with a bulky substitution group so that steric hindrance would block its adsorption on Lewis sites etc., or small enough for the complete determination of the total acidic and protonic sites. 2,6-di-t-butylpyridine may be a bulky enough molecule to try, as

was done by Dewing et al.(55). Another possible probe gas would be triphenylcarbinol which is believed to form the triphenylcarbonium ion upon dehydration by acidic catalyst (68,69). Due to the difference in their respective chemical shifts, they may yield interesting results.

Thirdly, carbon-13 NMR chemical shifts of the molecules when adsorbed on the surface, might be used quantitatively to determine the concentration of Bronsted and Lewis acidic sites on the surface. With the present results and derivations, we hope that it applies to other well-studied surfaces also.

Although the present results are satisfactory, they do, by no means, demonstrate that C-13 NMR spectroscopy is the perfect tool for surface study.

Another nucleus which is also suitable for this kind of study is N-15. It is less abundant and has a smaller gyromagnetic ratio than C-13, but with the pulse and Fourier transform technique we are using, it might

be possible. Chemical shift differences between NH_3 , coordinated NH_3, and NH_4^+ are given in ref.(70,71). Also their respective N-15 spectra are significantly different. Therefore, if we perform an N-15 experiment for NH_3 adsorbed on silica-alumina, we may be able to determine quantitatively the amount of NH_3 behaving as coordinately-bound and those as protonated species. Thus the concentration of acidic sites could be determined.

Nevertheless, the feasibility is limited by the fact that adsorbed NH_3 molecules may exchange between different sites, so the average of an original quartet and a quintet would be a mess, and only after some complicated analysis of line-shape would result a clear distinction.

While the above sounds reasonable, there are a few technical problems. First, for such a study to be a success, it requires quite a lot of NMR machine and computer time. Enriched $^{15}NH_3$ is cheap, but N-15 enriched organic compounds e.g. pyridine are expensive. Secondly, coordinately bound NH_3 has a partial positive charge and

the chemical shift of this species would be very close to that of NH_4^+, thus complicating the spectrum. Thirdly, due to the small size of NH_3 , it may not be able to differentiate the possible steric hindrance sites on the surface. Use of larger nitrogen-containing compounds may result in a more complicated NMR spectrum, except possibly, compounds like $N(CH_3)_3$ and $N(C_2H_5)_3$.

In the case of our present study, enriched C-13 compounds may solve the problem of peak assignments and positions and enhance the signal/noise ratio.

With the advent of solid-NMR and Proton-Enhanced Nuclear Induction Spectroscopy experiments, surface studies could be extended for cases in which stronger interactions occur. These studies are in progress in this laboratory at this time.

Bibliography

1) R. P. Bell, Acids and Bases, p.5, Mathuen (1952).

2) E. C. Franklin, Am. Chem. J. 20, 820 (1898); 47, 285 (1912); J. Am. Chem. Soc. 27, 820 (1905); 46, 2137 (1924).

3) J. N. Bronsted, Rec. Trav. Chim. 42, 718 (1923); J. Phys. Chem. 30, 377 (1926); Chem. Rev. 5, 231, 284 (1928); Z. Phys. Chem. 52, A169 (1934).

4) A. F. O. Germann, J. Am. Chem. Soc. 47, 2461 (1925).

5) G. N. Lewis, J. Franklin Inst. 226, 293 (1938); "Valence and Structures of Atoms and Molecules", Chemical Catalog Co. (1923).

6) M. Ussanowitch, J. Gen. Chem. USSR (Eng. Transl.) 9, 182 (1939); H. Gehlen, Z. Phys. Chem. 203, 125 (1954).

7) J. Bjerrum, Fys. Tidssk. 48, 1 (1950); B. Sansoni, Naturwissenschaften 38, 461 (1951).

8) R. E. Johnson, T. H. Norris and J. L. Huston, J. Am. Chem. Soc. 73, 3052 (1951).

9) H. Lux, Z. Elektrochem. 45, 303 (1939); H. Flood and T. Forland, Acta Chem. Scand. 1, 592, 781 (1947); J. W. Tomlinson, "The Physical Chemistry of Melts" (A symposium on molten slags and salts) p.22, Institution of Mining and Metallurgy (1953).

10) A. I. Shatenshtein, Adv. Physical Org. Chem. 1, 174 Acad. Press (1963).

11) R. G. Pearson, J. Am. Chem. Soc. 85, 3533 (1963).

12) K. Tanabe, "Solid Acids and Bases" Acad. Press (1970).

13) C. Prater and R. Lago, Adv. Catal. 8, 294, Acad. Press (1956).

14) C. Naccache et al., Proc. 3rd Int, Cong. Catal. 2 113 (1964).

15) J. Perri, ibid. 2, 1100 (1964).

16) I. Chapman and M. Hair, ibid. 2, 1091 (1964).

17) I. D. Gay and S. Liang, J. Catal. 44, 306 (1976).

18) R. J. Pugmire and D. M. Grant, J. Am. Chem. Soc. 90, 697 (1968).

19) D. K. Lavallee, M. D. Baughman and M. P. Phillips, J. Am. Chem. Soc. 99, 718 (1977).

20) P. C. Lauterbur, J. Chem. Phys. 43, 360 (1965).

21) H. L. Retcofsky and R. A. Freidel, J. Phys. Chem. 71, 3592 (1967).

22) E. Parry, J. Catal. 2, 371 (1963).

23) M. Tamele, Discussion Farad. Soc. 8, 270 (1950).

24) R. Hansford, Adv. Catal. 4, 17 (1953) Acad. press.

25) C. Planck, J. Colloid Sci. 2, 413 (1947).

26) C. L. Thomas, Ind. Eng. Chem. 41, 2564 (1949).

27) H. Bansei, J. Phys. Chem. 61, 970 (1957).

28) M. Basila and T. Kantner, J. Phys. Chem. 68, 3197 (1964); M. Basila, T. Kantner and K. Rhee, J. Phys. Chem. 70, 1681 (1966).

29) Y. Trambouze, J. Chem. Phys. 51, 723 (1954).

30) M. Basila and T. Kantner, J. Phys. Chem. 71, 467 (1967).

31) W. Hall, H. P. Leftin, F. J. Cheselske and D. E. O'Reilly, J. Catal. 2, 506 (1963).

32) L. Schreiber and R. Vaughan, J. Catal. 40, 226 (1975).

33) N. Bloembergen, E. Purcell and R. Pound, Phys. Rev. 73, 679 (1948).

34) R. Spooner and P. Selwood, J. Am. Chem. Soc. 71, 2184 (1949).

35) J. Zimmerman, B. Holmes and J. Lasater, J. Phys. Chem. 60, 1157 (1956).

36) C. P. Slichter, "Principles of Magnetic Resonance" Harper & Row, New York (1963).

37) F. Bloch, Phys. Rev. 70, 460 (1946); F. Bloch, W. W. Hansen and M. Packard, ibid. 70, 476 (1946).

38) J. Emsley, J. Feeney and L. Sutcliffe, "High Resolution Nuclear Magnetic Resonance Spectroscopy" vol.1 & 2, Pergamon Press (1965).

39) A. Abragam, "The Principles of Nuclear Magnetism" Oxford Press (1961).

40) H. A. Resing, "Advance in Molecular Relaxation Process", 1, 109, Elsevier Publishing Co. Amsterdam (1968).

41) H. Pfeifer, "NMR---Basic Principles and Progress" 7, Springer-Verlag, New York (1972).

42) A. G. Whitney, Ph.D. Thesis, Simon Fraser University. (1975).

43) T. C. Farrar and E. D. Becker, "Pulse and Fourier Transform NMR" Acad. Press (1971).

44) K. F. Kuhlmann and D. M. Grant, J. Am. Chem. Soc. 90, 7355 (1968); K. F. Kuhlmann, D. M. Grant and P. K. Harris, J. Chem. Phys. 52, 3439 (1970);

D. M. Grant and T. D. Alger, J. Phys. Chem. 75, 2539 (1971); Y. R. Lyerla, D. M. Grant and P. K. Harris, J. Phys. Chem. 75, 585 (1971).

45) A. Allerhand, D. Doddrell and R. Komoroski, J. Chem. Phys. 55, 189 (1971).

46) D. Michel, Surf. Sci. 42, 453 (1973).

47) J. F. Kriz and I. D. Gay, J. Phys. Chem. 80, 2951 (1976).

48) B. Rakvin and J. Herak, J. Mag. Res. 13, 94 (1974).

49) J. H. Van Vleck, Phys. Rev. 74, 1168 (1948).

50) J. E. Sarneski, H. L. Suprenant, F. K. Molen and C. N. Reilly, Analyt. Chem. 47, 2116 (1975).

51) J. B. Stothers, "Carbon-13 NMR Spectroscopy" Acad. Press (1972).

52) I. D. Gay and J. F. Kriz, J. Phys. Chem. 79, 2145 (1975).

53) I. D. Gay, J. Catal. 48,430 (1977).

54) K. A. K. Ebraheem, G. A. Webb and M. Witanowski, Org. Mag. Res. 11, 27 (1978).

55) J. Dewing, G. T. Monks and B. Youll, J. Catal. 44, 226 (1976).

56) H. A. Bensei, J. Catal. 28, 176 (1973).

57) H. Krezinger and H. Stolz, Ber. Bunsenges. Phys. Chem. 75, 1055 (1971).

58) L. H. Little, "Infrared Spectra of Adsorbed Molecules", Acad. Press (1968).

59) M. L. Hair, "Infrared Spectroscopy in Surface Chemistry", Marcel Dekker, New York (1967).

60) V. Holm and A. Clark, J. Catal. 2, 16 (1963).

61) J. A. Schwarz, J. Vac. Sci. Tech. 12, 321 (1975).

62) P. O. Scokart, F. D. Declerck, R. E. Semples and P. G. Rouxhet, J. Chem. Soc. Farad. I, 73, 359 (1977).

63) K. H. Bourne, F. R. Cannings and R. C. Pitkethly, J. Phys. Chem. 74, 2197 (1970).

64) J. P. Damon, B. Delmon and J. M. Bonnier, J. Chem Soc. Farad. I, 73, 372 (1977).

65) R. J. Cushley, D. Naugler and C. Ortiz, Can. J. Chem. 53, 3419 (1975).

66) F. E. Kiviat and L. Petrakis, J. Phys. Chem. 77, 1232 (1973).

67) W. M. Litchman, J. Mag. Res. 14, 286 (1974).

68) L. N. Izmailova and E. I. Kotov, Kinetika i Kataliz 18, 488 (1977).

69) Y. Yamamoto and H. Yamada, Chem. Letter, Chemical Soc. Japan 933 (1977).

70) E. F. Mooney and M. A. Qaseem, J. Inorg. Nucl. Chem. 30, 1439 (1968).

71) M. Witanowski and G. A. Webb, "Nitrogen NMR" Plenum Press (1973).